Extracellular matrix mechanics regulate transfection and SOX9-directed differentiation of mesenchymal stem cells

Adriana M. Ledo[a], Kyle H. Vining[b], Maria J. Alonso[a], Marcos Garcia-Fuentes[a] and David J. Mooney[b]

[a] Department of Pharmacy and Pharmaceutical Technology, IDIS Research Institute, CIMUS Research Institute, University of Santiago de Compostela, 15782 Santiago de Compostela, Spain
[b] Wyss Institute for Biologically Inspired Engineering and John A. Paulson School of Engineering and Applied Sciences, Harvard University, Cambridge, Massachusetts 02138, USA

Correspondence should be addressed to M.G.F. (marcos.garcia@usc.es) and D.J.M (mooneyd@seas.harvard.edu):

Prof. Marcos García Fuentes: BiDD Group, CiMUS research center, Universidad de Santiago de Compostela, Spain, (+34) 881815450

Prof. David J. Mooney: Robert P. Pinkas Family Professor of Bioengineering at Harvard University, USA, (617) 384-9624

Other contact details are as follows:

Adriana M. Ledo: adriana.martinez_ledo@novartis.com

Kyle H. Vining: kvining@g.harvard.edu

Maria J Alonso: mariaj.alonso@usc.es

ABSTRACT

Gene delivery within hydrogel matrices can potentially direct mesenchymal stem cells (MSCs) towards a chondrogenic fate to promote regeneration of cartilage. Here, we investigated whether the mechanical properties of the hydrogel containing the gene delivery systems could enhance transfection and chondrogenic programming of primary human bone marrow-derived MSCs. We developed collagen-I-alginate interpenetrating polymer network hydrogels with tunable stiffness and adhesion properties. The hydrogels were activated with nanocomplexed SOX9 polynucleotides to direct chondrogenic differentiation of MSCs. MSCs transfected within the hydrogels showed higher expression of chondrogenic markers compared to MSCs transfected in 2D prior to encapsulation. The nanocomplex uptake and resulting expression of transfected SOX9 were jointly enhanced by increased stiffness and cell-adhesion ligand density in the hydrogels. Further, transfection of SOX9 effectively induced MSCs chondrogenesis and reduced markers of hypertrophy compared to control matrices. These findings highlight the importance of matrix stiffness and adhesion as design parameters in gene-activated matrices for regenerative medicine.

Key words: GAMs, IPNs, 3D transfection, SOX9, tissue engineering

1. Introduction

Directing differentiation of stem cells is a promising approach in regenerative medicine,(Merrell and Stanger 2016; Jopling, Boue, and Belmonte 2011) in order to generate specified cells to restore missing, damaged, or diseased tissue.(Murry and Keller 2008; Yamamizu et al. 2013) Several autologous and allogeneic stem cell products are available (i. e. Holoclar, Tigenix,, Temcell, Allocord) but existing therapies on the market mainly utilize growth factors delivered from polymer matrices to promote differentiation of tissue-resident stem cells.(Yannas et al. 1989; Lo et al. 2012) Limitations of these devices include the necessity of using high doses of growth factors together with a poor control over their release kinetics, which potentially can lead to side effects and complications.(Kang, Hsu, and Lehman 2017; Epstein 2013; DeVine et al. 2012) Gene therapy approaches based on viral vectors have been recently commercialized and could address problems of protein stability and dosing, but they pose concerns in terms of immunogenicity and integration-mediated genotoxicity.(D. Wang, Tai, and Gao 2019)

Hydrogels may aid in overcoming the limitations of protein-based regenerative strategies and viral vector approaches by delivering polynucleotides in a tissue-conductive three-dimensional (3D) environment, while inducing prolonged expression of growth factors and transcription factors that regulate tissue development.(Im, Kim, and Lee 2011; Raisin, Belamie, and Morille 2016) Known as Gene-Activated Matrices (GAMs), the first and more studied examples were based on the delivery of plasmid DNA (pDNA) or viral vectors. Recently, mRNA has been used for GAM activation providing enhanced transfection efficiency.(Elangovan et al. 2015; Balmayor et al. 2016; Khorsand et al. 2017) In either case, the effects of the hydrogel matrix itself remain to be considered. Previous studies on gene transfer on two-dimensional (2D) substrates have demonstrated that both material stiffness(Kong et al. 2005) and adhesion properties,(Y. A. Wang et al. 2007) as well as the presence of ECM proteins can modulate transfection.(Dhaliwal et al. 2010; Perlstein et al. 2003) Yet, conclusions obtained from 2D studies do not always translate to 3D systems(Chu and Kong 2012; Shepard et al. 2010; Dhaliwal, Oshita, and Segura 2013; Lei, Padmashali, and Andreadis 2009) due to the higher complexity of cell transfection within these environments.(Zhang et al. 2012, 2010) Moreover, the mechanical properties of GAMs may modulate the biological effect of the induced transgene, because cell fate can also be regulated intrinsically by stiffness, elasticity, and stress-relaxation.(Engler et al. 2006; Guilak, Cohen, and Estes 2009; Chaudhuri, Gu, Darnell, et al. 2015; Huebsch et al. 2010; Vining and Mooney 2017)

Here, we investigated whether imparting specific mechanical properties to a GAM environment can enhance 3D gene transfer and support chondrogenesis. To this end, we developed a set of interpenetrating polymer networks (IPNs) of collagen-I and alginate. With these IPNs, it is possible to independently tune the stiffness of the matrix, without significantly affecting its architecture, polymer concentration and adhesion ligand density.(Branco da Cunha et al. 2014) In addition, their composition resembles that of the native cartilaginous tissue(Nathaniel, Mow, and Foster 1998; Hardin, Cobelli, and Santambrogio 2015) and they could yield more realistic ECM models compared to biologically inert polymer hydrogels that present synthetic adhesion

ligands.(Balakrishnan and Banerjee 2011; Hinderer, Layland, and Schenke-Layland 2016) We designed GAMs with tunable stiffness and cell-adhesion ligand densities and studied their capacity to promote the transfection of SOX9, a pivotal transcription factor in chondrogenesis.(Dy et al. 2012; Bi et al. 1999) IPN stiffness was modulated by changing the amount of the alginate crosslinking agent (i.e. calcium carbonate nanoparticles), while adhesion ligand density was tuned by modifying the weight ratio between alginate (lacking cell adhesion ligands) and collagen (with numerous integrin-binding domains). We characterized the effect of GAM mechanics on SOX9 expression kinetics and nanocomplex internalization and compared the expression levels of chondrogenic markers with those obtained after 2D transfection. These results show how hydrogels can be used to enhance non-viral gene delivery and optimize GAMs for use in regenerative medicine.

2. Materials and methods

2.1 Cell culture

Human adipose derived Mesenchymal Stem Cells (MSCs) and human bone marrow derived MSCs were acquired from ATCC and isolated from fresh unprocessed bone marrow (Lonza), respectively. Briefly, bone marrow samples were diluted in cold PBS pH 7.2 (Gibco) supplemented with 2% v/v heat inactivated fetal bovine serum (Gibco) and filtered (pore size 100 µm). Then, the diluted cell suspension was added over Lymphoprep (Stemcell Technologies) and centrifuged (800xg, 30 min, 20°C) yielding an interphase of mononuclear cells. CD14 microbeads (Miltenyi Biotech) were used for the depletion of CD14+ cells by magnetic separation and MSCs were allowed to adhere to tissue culture flasks. MSCs were cultured in α-MEM (Gibco) supplemented with 10 ng/ml rhFGF basic (Peprotech), 1% penicillin-streptomycin (Gibco) and 10% (adipose MSCs,) or 20% (bone marrow MSCs) heat inactivated fetal bovine serum. Cells were detached from the plates using TrypLE enzyme solution (Gibco) and plated at 5000-7500 cells/cm^2. Media was changed every 2-3 days and cells were split at 70-80% confluency. For experiments involving ROCK inhibition, Y-27632 was added to cell culture media at 10 µM.

2.2 Plasmid design and mRNA synthesis

SOX9 plasmid was designed to enable optimal mRNA synthesis by in vitro transcription (IVT) (**Fig. S1**). To construct the plasmid, the SOX9 CDS, a Kozak consensus sequence and the 3' UTR of the α globin gene(Kozak 1987; Holcik and Liebhaber 1997; Warren et al. 2010) were synthesized and cloned into a pCMVTnT expression vector (Promega, Madison, WI, USA) by Genewiz (South Plainfield, NJ, USA). The plasmid was sequence-verified (Stab Vida, Caparica, Portugal) and transformed into DH5α *E. Coli* bacteria for its propagation. Extraction of the plasmid from the bacterial cultures was performed with the NucleoSpin Plasmid Kit (Macherey-Nagel, Dueren, Germany) according to the manufacturer's instructions. SOX9 plasmid was used as template to synthesize SOX9 mRNA using the mMESSAGE mMACHINE T7 Ultra kit (Ambion, Foster City, CA, USA) following the manufacturer's protocol. Briefly, SOX9 plasmid was linearized using BamHI restriction enzyme (Promega) and 2-7 enzyme units per µg of pDNA. Endonuclease digestion was confirmed by gel electrophoresis and 1.35 µg of linearized plasmid was used as template for each 20 µl reaction. mRNA was purified via phenol-chloroform extraction using Phase Lock 1.5 ml tubes (5 Prime, Hilden, Germany) followed by ethanol

precipitation and quantification by Nanodrop (Thermo Fisher Scientific, Waltham, MA, USA).

2.3 Preparation of 3DFectIN complexes

For 3D transfection experiments, 25 µl of transfection complexes were prepared per 150 µl of total IPN mix. Complexes were assembled in OptiMEM (Gibco) at 3:1 3DFectIN:pDNA/mRNA ratio (µl:µg), following the manufacturer's instructions. Briefly, a solution containing 1.5 µg of SOX9 pDNA/mRNA was added over a solution containing 4.5 µl of 3DFectIN reagent (OZ Biosciences) in a 1/1 v/v ratio, mixed by pipetting up-down and incubated for 20 min at room temperature. To investigate the distribution of the complexes within the IPNs, SYBRGold-labeled pDNA complexes were prepared. A pDNA aqueous solution was labeled by mixing with a 50X DMSO solution of SYBR®Gold Nucleic Acid Gel Stain (Invitrogen) in a ratio 1:1 (µg:µl) and incubated for 5 min at room temperature before complex formation. Complexes were then encapsulated within the IPNs and visualized under fluorescence microscopy (EVOS FL Cell Imaging system).

2.4 IPNs preparation

Low viscosity, low MW sodium alginate was purchased from Pronova (UP VLVG). Before its use, alginate was dialyzed against deionized water for 2 days (3.5 kDa cutoff) and lyophilized. Dry alginate was then reconstituted at 8.0% w/v in Hank's Balanced Salt Solution with HEPES (HBSS, 20 mM HEPES) without calcium and magnesium prior to IPN formation. Ice-cold bovine collagen type-I (Advanced Biomatrix) was mixed with 1 M HEPES and 10X HBSS solutions at 1:50 and 1:10 v/v ratios to the amount of collagen needed, respectively, and pH was adjusted to 7.4 with NaOH 1 M. Calcium carbonate nanoparticles (nano-PCC, Multifex-MM, Specialty Minerals) were encapsulated within the IPNs to crosslink the alginate, and Ca^{2+} release was triggered by a media acidification induced by the addition of glucono delta-lactone (GDL). Before encapsulation, nanoparticles were suspended in RNase free water (Invitrogen) at 1% w/v, sonicated for 15 s at 70% amplitude and 4 °C (Branson Sonifier) and maintained under magnetic stirring to prevent sedimentation. GDL (Merck) was dissolved in HBSS (4% w/v) and incorporated to the IPN mix at a fourfold molar excess with respect to calcium, immediately before IPN molding. For transfection experiments, pDNA and mRNA complexes were prepared as previously described (2.2) and mixed with hMSCs prior to their encapsulation within the IPNs, yielding the GAMs. hMSCs were suspended at 22.5 x 10^6 cells/ml in OptiMEM and added to the IPN at a density of 1.5 x 10^6 cells/ml.
All the different components were blended in 2 ml glass vials placed on an ice bath under magnetic stirring. HBSS supplemented with 20 mM HEPES was added first to reach the final volume of IPN mix. This buffer was supplemented with NaOH to yield a 7 mM concentration of NaOH in the final mix. The ice-cold collagen solution was then included, and while it was stirring, transfection complexes were mixed with hMSCs by pipetting up-down and then added to the collagen solution. Once this mix was homogeneous, calcium carbonate nanoparticles were incorporated, followed by the addition of alginate. Finally, the solution of GDL was added and IPNs were casted in 96 or 48 well plates (Thermo Fisher Scientific). IPNs were then allowed to gel for 30 min at room temperature (alginate crosslinking) and 30 min at 37 °C (collagen crosslinking). Due to the drop in pH caused by the hydrolysis of GDL, pH was balanced by the addition of HBSS 20 mM HEPES during the first 4h after IPN crosslinking. Once pH was stabilized, culture media was added on top of the IPNs. Culture media was refreshed every 2-3 days.

2.5 Mechanical Characterization of IPNs

IPN mechanical properties were characterized with an AR-G2 stress controlled rheometer (TA Instruments). IPNs without cells and gene complexes were prepared as described above and placed onto the surface plate of the rheometer immediately before gelation. Right after, a 20 mm 2° aluminum cone was put into contact with the IPN creating a 20 mm gel disk. To prevent sample dehydration, the exposed gel surfaces within the rheometer geometry were surrounded with a wet Kimwipe, and 800 µl of HBSS were carefully added after the first step of IPN gelation. IPNs were allowed to gel at 25 °C for 30 min (alginate crosslinking) followed by 30 min of collagen crosslinking at 37 °C, and mechanical properties were measured over time as previously described(Chaudhuri et al. 2014). The storage modulus at 1% strain and 1 Hz was recorded periodically until it reached its equilibrium value (30-60 min). Then, a strain sweep (0.1-20% strain) was performed to confirm this value was within the linear elastic regime, followed by a frequency sweep (0.1-10 Hz). No pre-stress was applied to the IPNs for these measurements. For stress-relaxation measurements, strain was raised during 1 s to 15% and then held constant, while the load was recorded as a function of time. Both the sweeps and stress-relaxation analysis were performed at 37 °C.

2.6 Cell retrieval for gene expression and flow cytometry analysis

At the desired time points, cells were retrieved from the GAMs before RNA extraction and fluorocytometric analysis. Media was aspirated and GAMs were washed twice with PBS (Gibco). GAMs were then removed from the plates with a spatula and placed in 1.5 ml tubes before a two-step enzymatic digestion. Fresh enzyme solutions were prepared in Ca^{2+}, Mg^{2+} PBS (Gibco) supplemented with 1% w/v bovine serum albumin (Sigma). In a first step, 350 µl of a solution containing 34 U/ml alginate lyase (Sigma) and 300 U/ml collagenase type I (Gibco) were added per 200 µl of GAMs and incubated for 15 min at 37 °C under horizontal shaking (300 rpm, Heidolph Titramax platform shaker). Next, samples were centrifuged (5 min, 400xg) and the enzyme solution was removed. A second digestion was performed with 350 µl of a solution containing 300 U/ml collagenase and GAMs were further incubated for 15 min and centrifuged to discard the collagenase solution. For RNA extraction, the resulting pellet was mixed with 1 ml of 0.05M ice cold EDTA by pipetting up-down and then centrifuged again. This step was omitted for flow cytometry samples. Finally, the cell pellet was washed with 1 ml ice cold PBS and placed on ice until further analysis.

Total RNA was extracted with the SPEEDTOOLS total RNA extraction kit (Biotools) following the manufacturer's instructions. RNA concentration was quantified using a Nanodrop 2000 spectrophotometer (Thermo Fisher Scientific).

2.7 Uptake studies

Uptake of the transfection complexes within the GAMs was evaluated using a Cy5-labeled pDNA. For this, pcDNA3.1(+) (Addgene) was labeled with the Cy®5 *Label* IT® Tracker™ kit (Mirus) following the manufacturer's instructions and subsequently loaded in the transfection complexes. Complexes were then encapsulated within the GAMs together with MSCs and cultured for different lengths of time, after which cells were analyzed via flow cytometry and confocal microscopy. For flow cytometry analysis, MSCs were retrieved from the GAMs as previously described (section 2.5) and analyzed on a BD FACSCalibur. Cells were gated to eliminate interferences from remaining traces of polymers (**Fig. S2**) and the percentage of Cy5+ cells among the gated population was quantified. To evaluate the uptake via confocal microscopy, GAMs were cultured on glass coverslips. At the time of analysis, MSCs were fixed in 10% buffered formalin for 20 min at room temperature followed by permeabilization with Triton X-100 (0.2% v/v in

PBS) for 10 min. Cells were then stained with DAPI (Sigma-Aldrich) and Alexa Fluor™ 488 Phalloidin (Thermo Fisher Scientific) and imaged on a Leica TCS SP5 confocal microscope. Cy5 Raw Fluorescence Intensity (RFI) per cell was quantified using ImageJ software after selecting the cell contours in the corresponding confocal images.

2.8 cDNA synthesis and qRT-PCR

Reverse transcription was carried out using 100-500 ng of total RNA per sample in a 30 µl final reaction volume. First, total RNA was mixed with random primers and dNTPs (Invitrogen) and kept at 65 °C for 5 min. Samples were then incubated with a mix of RNase OUT, 5x first strand buffer and DTT (Invitrogen) for 2 min at 37 °C and subsequently placed on ice. Finally, reverse transcriptase (M-MLV, Invitrogen) was included and the cycle was continued as follows: 10 min at 25 °C, 50 min at 37 °C and 15 min at 70 °C. The resulting cDNA (5-10 ng) was used to assemble qRT-PCR reactions in a final volume of 20 µl containing Universal PCR Mastermix and TaqMan assays (Applied Biosystems, **Table S1**). The thermal cycling was done in a StepOne Real Time PCR System (Applied Biosystems) performing a 10 min hold at 95 °C followed by 40 cycles of 15 sec at 95 °C and 1 min at 60 °C. Gene expression values were normalized to internal controls (Actin β and GAPDH) and presented either as the $\log_2(\Delta Ct)$ or the fold change relative to cells plated in 2D before the experiments using the comparative $2^{-\Delta\Delta Ct}$ method.(Pfaffl 2001)

2.9 Chondrogenic differentiation

Chondrogenesis experiments were performed with adipose hMSCs below passage 10. IPNs (200 µl) were casted in 48 well plates and cultured for 21 days in Complete Chondrogenic Medium (CCM) consisting of DMEM high-glucose 1 mM pyruvate (Gibco), 100 nM dexamethasone (Sigma-Aldrich), 50 µg/ml ascorbic acid 2-phosphate (Sigma-Aldrich), 40 µg/ml L-proline (Sigma-Aldrich), 1% ITS Premix supplement (Becton Dickinson), 1% penicillin/streptomycin (Gibco) and 10 ng/ml transforming growth factor-β3 (Peprotech). Media was replaced every 2 days in all experiments. GAMs were activated with 2 µg of SOX9 mRNA per GAM, and their chondrogenic potential was compared to non-activated matrices. At the end of the experiments, GAMs were retrieved for analysis. Gene expression of chondrogenic markers *SOX9*, aggrecan (*ACAN*), collagen type-II (*COL2A1*) and collagen type-X (*COLX*) was assessed by qRT-PCR. SOX9, aggrecan and collagen type-X were also detected by immunohistochemistry (IHC).

2.10 Immunohistochemistry

GAMs were retrieved from tissue culture plates, washed with PBS twice and fixed with 10% buffered formalin at room temperature for less than 24 h. After fixation, samples were maintained in 70% ethanol until dehydration and paraffin sectioning. Sections of 4 µm thickness were cut and allowed to adhere to poly-L-lysine treated glass slides overnight at 55 °C. Before staining, sections were dewaxed in xylene and hydrated with graded ethanol, and antigens were retrieved in Tris-EDTA buffer during 20 min at 95 °C (PT Link, Agilent). Samples were pretreated with hydrogen peroxide and blocked with serum free protein block (Dako; Agilent) before incubation with primary antibodies against SOX9 (ab5535, Merck), aggrecan (ab3778, Abcam), and collagen type-X (ab49945, Abcam). Primary antibodies were diluted in antibody diluent (Dako) at 1:500 (SOX9), 1:100 (aggrecan) and 1:1000 (collagen type-X) and incubated overnight at 4 °C. Then, samples were incubated with goat secondary antibodies labeled with HRP (Dako) at 1:100 for 1 h and stained with 3,3'-diaminobenzidine (DAB). Negative controls were

obtained by omitting the primary antibodies (**Fig. S3**). All samples were observed using an Olympus BX43 microscope equipped with an Olympus XC50 camera. Mean Intensities were quantified with the IHC macro of the Fiji software(Schindelin et al. 2012) while the percentage of positive cells was calculated by dividing the number of stained cells by the total number of cells.

2.11 Statistical Analysis

The statistical analysis was performed using GraphPad Prism. Data were analyzed with either the D'Agostino & Pearson or the Shapiro-Wilk normality tests. Where applicable, data are reported as the mean ±SD. Data were compared using One-way ANOVA with Tukey's post-hoc multiple comparison test and unpaired two-tailed t tests and p-values less than 0.05 were considered to be statistically significant.

Results

3.1 Characterization of collagen-I-alginate interpenetrating networks (IPNs)

Collagen-I-alginate IPNs with tunable mechanical properties were prepared to investigate the influence of stiffness and adhesion properties on the transfection efficiency of gene-activated matrices (GAMs). To determine the effect of each property independently, we designed a set of IPNs that would allow us to change both variables separately. Analysis with oscillatory rheology was used to tune IPN stiffness based on $CaCO_3$ concentration, and four IPNs were fabricated with storage modulus (G') from 150 to 1500 Pa at a fixed frequency of 1 Hz and 1% strain after 60 min of gelation (**Fig. 1A), S4**). A strain sweep was performed to confirm the values were within the linear elastic regime (**Fig. S5**). Within this range of stiffness, we modulated cell-adhesion ligand density by adjusting the collagen:alginate w:w ratio from 1:1 to 1:10. In contrast to collagen, alginate presents no intrinsic integrin-binding domains for cells and hence, higher collagen:alginate ratios confer higher adhesion ligand density. Accordingly, the resulting IPN set can be divided in four groups: IPNs of low stiffness and very high cell-adhesion ligand density (Soft 1:1), IPNs of low stiffness and high adhesion ligand density (Soft 1:2), IPNs of high stiffness and high adhesion ligand density (Stiff 1:2) and IPNs of high stiffness and low adhesion ligand density (Stiff 1:10). The amount and distribution of collagen fibers across the IPN set was analyzed by confocal reflectance microscopy (**Fig. S6**). A significant reduction in collagen fibers was observed for the 1:10 condition, which is consistent with the lower percentage of collagen present in these IPNs (0.1 versus 0.5 wt% collagen). The two soft IPNs have the same collagen concentration (0.5 wt%) and showed the same fiber intensity. However, soft 1:1 IPNs have less alginate than soft 1:2 IPN (0.5 versus 1 wt% alginate) and thus a higher collagen-to-alginate ratio. The paired comparison between the different groups enabled us to explore the effect of stiffness (Soft 1:2 vs Stiff 1:2) and cell-adhesion ligand density (Soft 1:1 vs Soft 1:2 and Stiff 1:2 vs Stiff 1:10) on gene transfer efficiency (**Fig. 1B**).

Frequency dependent storage moduli were characterized over a frequency range of 0.1 to 1 Hz, and indicated that the IPNs exhibited some degree of viscoelasticity, as previously observed(Branco da Cunha et al. 2014) (**Fig. S5**). IPN viscoelasticity was further characterized by stress relaxation behavior, with half-times ($\tau_{1/2}$) of 10-300 s depending on the collagen:alginate ratio (**Fig. S7**). A stress relaxation half-time of 100 s is in agreement with previous results for low viscosity, low MW alginate gels, and has been identified as the optimum $\tau_{1/2}$ to allow cell-mediated gel remodeling,(Chaudhuri,

Gu, Klumpers, et al. 2015) which is necessary for regeneration of osteochondral tissues like cartilage.(H. P. Lee et al. 2017)

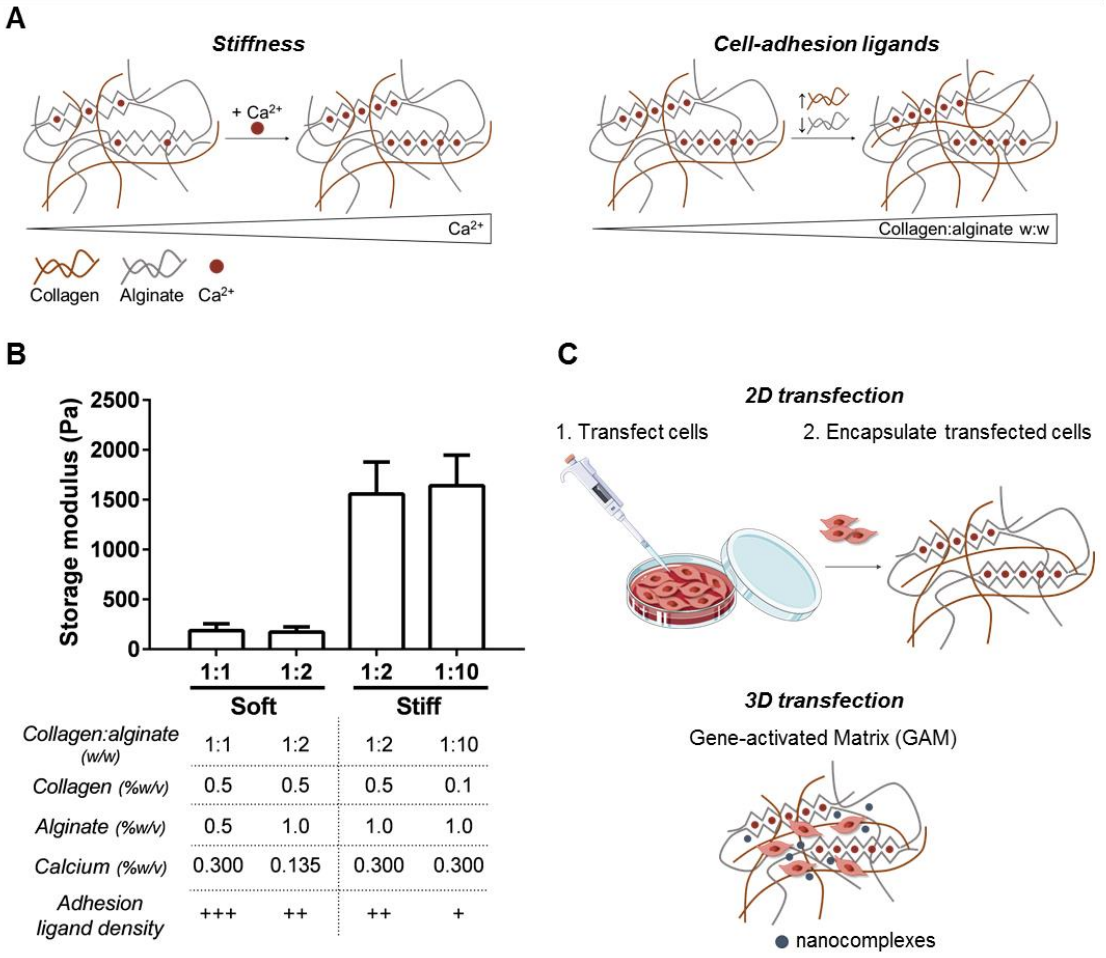

Collagen:alginate (w/w)	1:1	1:2	1:2	1:10
Collagen (%w/v)	0.5	0.5	0.5	0.1
Alginate (%w/v)	0.5	1.0	1.0	1.0
Calcium (%w/v)	0.300	0.135	0.300	0.300
Adhesion ligand density	+++	++	++	+

Figure 1. IPNs show tunable stiffness and cell-adhesion ligands and can be loaded with nanocomplexed polynucleotide molecules to generate Gene-Activated Matrices (GAMs). (A) Scheme showing the modulation of IPN mechanical properties through crosslinker concentration and polymer ratio. The IPN is illustrated as brown collagen fibers and grey alginate polymer chains. The calcium ions crosslinking the G-blocks of the alginate network (zig-zag structures) are shown as red dots. Objects are not drawn to scale. (B) Storage modulus at 1 Hz and 1% strain after 1 h of IPN crosslinking and detailed composition and properties of the IPN set. (C) Scheme showing the experimental setups used for the transfection assays.

3.2 Increased stiffness and cell-adhesion ligand density enhance IPN transfection efficiency

The transcription factor SOX9 has pivotal roles in chondrogenic lineage specification and has potential for the design of GAMs for cartilage regeneration. To prepare SOX9-GAMs, IPNs were loaded with nanocomplexed SOX9 sequences within the hydrogel matrix, as depicted in **Fig. 1C**, and their transfection efficiency was assessed. In order to determine the role of cell encapsulation and matrix mechanics on SOX9 expression, we compared the direct transfection of bone marrow MSCs in GAMs with 1) the encapsulation of MSCs

in blank IPNs and 2) the transfection of MSCs in 2D and subsequent encapsulation in blank IPNs.

In a first step, bone marrow MSCs were encapsulated in blank IPNs and SOX9 expression was assessed to discard any potential inherent effect of matrix mechanics on SOX9 expression that would impact the transfection results (**Fig. S8**). In a second step, MSCs were transfected in 2D and then encapsulated within the polymer matrices in order to evaluate whether this encapsulation was able to alter transgene expression levels. To this end, SOX9 pDNA transfections were performed with the commercial reagent Lipofectamine® 2000 and transfected cells were loaded within the IPNs after retrieval from 2D. qRT-PCR analysis revealed that MSCs encapsulated in the IPNs exhibited a higher SOX9 expression relative to the cells after 2D transfection, which indicates some degree of cell transfection occurs within the gels (**Fig. 2A**), and we hypothesized that remaining pDNA complexes from 2D transfection were encapsulated along with the cells in the IPNs. To examine this hypothesis, Lipofectamine® complexes were loaded with Cy5-labeled pDNA and observed during 2D transfection by fluorescence microscopy, which showed that pDNA complexes remained adhered to the cells even after retrieval by enzymatic separation (**Fig. S9**). This result confirms that residual complexes were encapsulated within the IPNs together with the cells, and thus 3D transfection was likely occurring. The same result was not observed when 2D transfections were performed with mRNA (**Fig. S8**), most likely due to the lower stability of mRNA sequences, further confirming that 3D transfection of remaining pDNA complexes was occurring. In these experiments, IPNs of high stiffness promoted the highest fold increase in SOX9 expression, suggesting that IPN mechanics can modulate transfection (**Fig. 2A**).

To specifically determine the role of mechanics on 3D transfection, SOX9 pDNA sequences were first nanocomplexed with 3DFectIN® and subsequently loaded into the IPNs to prepare SOX9 GAMs. Compared to Lipofectamine® 2000, 3DFectIN® is optimized for transfection within 3D environments and hence the encapsulation of MSCs within these GAMs promoted their 3D transfection by overexpression of SOX9. In agreement with the previous results, qRT-PCR data showed a higher SOX9 expression in matrices of higher stiffness. Additionally, lower collagen:alginate ratios were associated with reduced gene transfer efficiency (**Fig. 2B**). In the case of stiff GAMs, where the collagen:alginate ratio was modulated from 1:2 to 1:10, this negative impact was found to correlate to an increased destabilization of the nanocomplexes with lower collagen:alginate ratios (**Fig. S10**). For soft GAMs, changing collagen:alginate ratio from 1:1 to 1:2 did not induce nanocomplex aggregation (**Fig. S10**), but resulted in a dramatic decrease in SOX9 levels. Soft 1:1 and soft 1:2 IPNs differ in the collagen:alginate ratio but also in the amount of calcium carbonate particles used in their fabrication. Given that inorganic calcium-based particles have been used as complexation reagents for polynucleotides, we performed two control experiments in order to rule out their contribution to the higher transfection efficiency of 1:1 IPNs. We confirmed that the excess of calcium ions did not improve lipoplex transfection efficiency of MSCs plated in 2D (**Fig. S10**). In this regard, it's worth mentioning that the calcium carbonate particles are dissolved by glucono delta-lactone during IPN gelation, so one would not expect their effects would persist during transfection. In order to test the effect of adhesion ligands on transfection efficiency, transfection in soft 1:1 IPNs (0.5% collagen, 0.5% alginate, 0.3% calcium carbonate) was compared with a plain 0.5% collagen-only gel. The collagen gel resulted in higher SOX9 expression, which is consistent with higher transfection in the soft 1:1 IPNs that have a higher amount of collagen relative to alginate. We suggest increased collagen ligands of collagen-only or soft 1:1 IPNs promote transfection compared to soft 1:2 IPNs, due to higher availability of adhesive ligands, rather than the presence of calcium carbonate particles (**Fig. S11**).

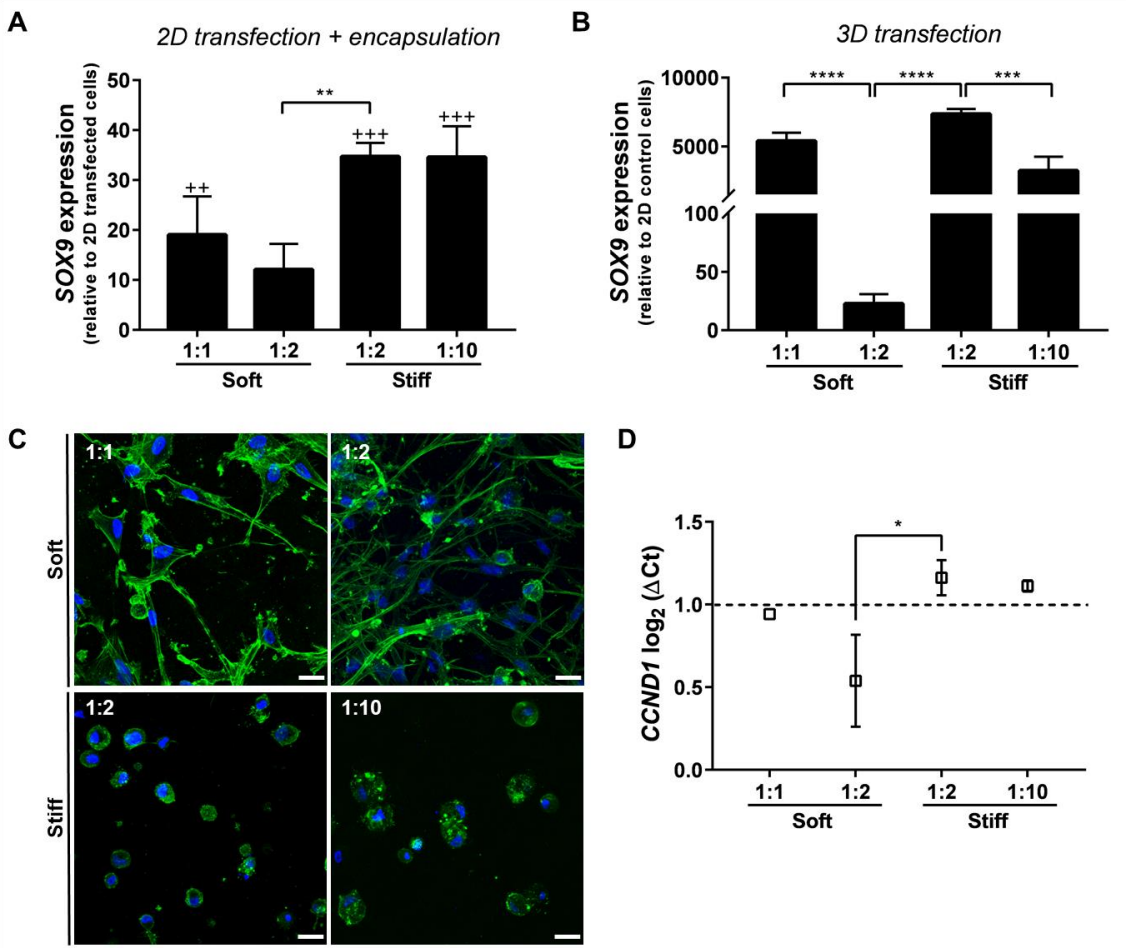

Figure 2. Matrix stiffness and adhesion exert a positive effect on bone marrow MSC transfection. (A) *SOX9* overexpression 48 h after encapsulation of pDNA-transfected cells within the IPNs. Gene expression levels were normalized to *GAPDH* and presented as relative to the levels in 2D transfected cells before encapsulation. One-way ANOVA with a Tukey's post-hoc multiple comparison test was performed to compare *SOX9* expression levels to the levels in transfected cells before encapsulation (++P≤0.01, +++P≤0.001, n=3) and between the IPNs (**P≤0.01, n=3). (B) *SOX9* expression 48 h after pDNA transfection within the Gene-activated Matrices (GAMs). Gene expression levels were normalized to *GAPDH* expression and compared to the levels in MSCs before encapsulation. One-way ANOVA with a Tukey's post-hoc multiple comparison test was performed to compare gene expression levels between the GAMs (***P≤0.001, ****P≤0.0001, n=3). (C) MSC morphology within the IPN set (F-actin in green, nuclei in blue). Scale bar = 25 µm for all the images. (D) qRT-PCR quantification of Cyclin D1 (*CCND1*) expression 48h after pDNA 3D transfection. Gene expression levels were normalized to *GAPDH* and expressed as $\log_2$ (ΔCts). The dotted line represents $\log_2$ (ΔCt) = 1, and is used to highlight the GAMs with higher *CCND1* levels. One-way ANOVA with a Tukey's post-hoc multiple comparison test was performed to compare gene expression levels between the GAMs (*P≤0.5, n=2). GAMs are described by their stiffness and collagen:alginate w:w ratios (1:1 to 1:10).

In accordance with previous studies, we observed that soft matrices promoted spread cell morphologies whereas stiff matrices resulted in rounded cell shapes(Branco da Cunha et al. 2014) (**Fig. 2C**). We hypothesized that efficient cell attachment might be necessary for cytoskeletal organization, which in turn could modify the intracellular transport of the complexes. Indeed, for both Soft 1:1 and Stiff 1:2 GAMs, transfection was affected by the state of cell cytoskeleton, as demonstrated by a decrease in SOX9 expression after the addition of the ROCK inhibitor Y-27632 (**Fig. S11**). Together with adhesion ligand density, gene transfer efficacy was also increased with stiffness, as evidenced by the differences between Soft 1:2 and Stiff 1:2 GAMs. Stiffness has been previously shown to promote transfection efficiency in 2D environments by increasing

cell proliferation.(Kong et al. 2005) Although an indirect measure of cell proliferation, higher transfection efficiencies were associated with upregulation of cyclin D1 (*CCND1*) gene expression, which regulates the cell cycle(Shepard et al. 2010; Gojgini, Tokatlian, and Segura 2011) (**Fig. 2D**).

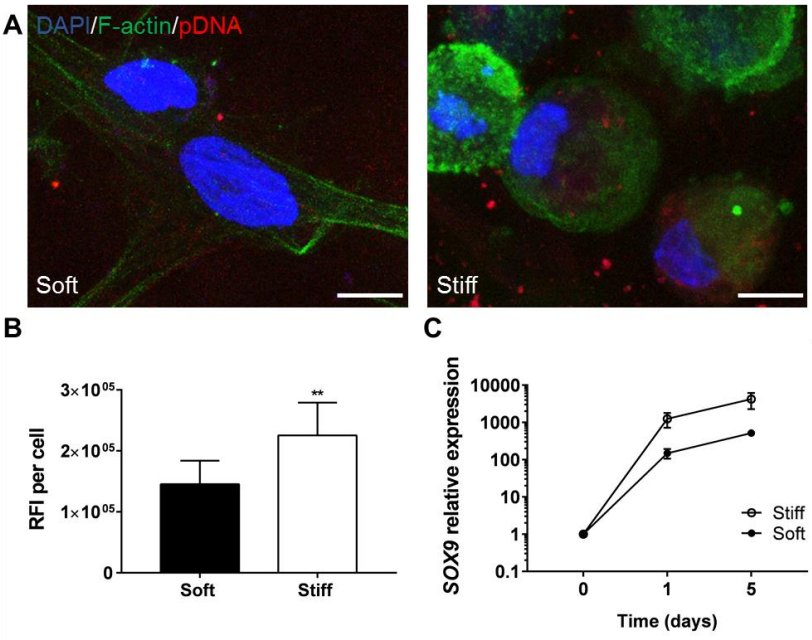

Figure 3. IPN stiffness increases the uptake of the pDNA nanocomplexes. (A) Confocal images of bone marrow MSCs within IPNs showing the localization of the pDNA nancomplexes. Scale bars = 10 µm for all the images. (B) Quantification of Raw Fluorescence Intensity (RFI) per cell of A) (Unpaired two-tailed t test, n =3, **P≤0.01). (C) *SOX9* expression kinetics after pDNA transfection within stiff and soft GAMs prepared with a 1:2 collagen:alginate w:w ratio. Gene expression levels were measured by qRT-PCR, normalized to *GAPDH* expression and compared to the levels in MSCs before encapsulation. See also Figure S12.

We next hypothesized that changes in transfection efficiency could be related to different cellular internalization rates of the nanocomplexes. Two GAMs with the same collagen:alginate ratio and different stiffness, soft 1:2 and stiff 1:2 GAMs, were selected to investigate this hypothesis. Transfection complexes were prepared with Cy5-labeled pDNA and their localization within the cells was tracked by confocal microscopy, and their amount was quantified by flow cytometry. As observed in **Figure 3A** and **3B**, stiff GAMs induced higher nanocomplex accumulation within the cells compared to soft GAMs. Accordingly, flow cytometry analysis also showed a higher Mean Fluorescence Intensity for bone marrow MSCs transfected within stiff GAMs (**Fig. S12**).

Further, analysis of the kinetics of transgene expression showed that stiff GAMs maintained over time higher SOX9 expression than soft GAMs (**Fig. 3C**). This suggests that the effects of GAM mechanics are maintained long-term, and consequently are an important parameter for the design of GAMs.

3.3 Chondrogenic differentiation of aMSCs is enhanced by transfection of SOX9 within stiff GAMs

We next determined if GAM properties could also impact chondrogenic differentiation induced by SOX9 overexpression. Given the influence of matrix mechanics on the

modulation of cell phenotype, we first determined whether stiffness affects chondrogenic differentiation. To this end, we encapsulated adipose MSCs within both stiff and soft 1:2 IPNs and subjected them to chondrogenic differentiation in the absence of SOX9 transfection. Additionally, in order to explore the effect of stiffness during SOX9 enforced expression, we transfected the cells in 2D with SOX9 lipoplexes prior to loading within soft and stiff IPNs and compared these Lipofected IPNs with the control (non-transfected) IPNs. mRNA sequences were used for these differentiation experiments instead of pDNA, due to their proven higher potency relative to pDNA.(Sahin, Karikó, and Türeci 2014)-(Warren et al. 2010)

As expected, SOX9-transfected MSCs showed higher levels of SOX9 mRNA expression compared to control (non-transfected) cells (**Fig. 4A**) after encapsulation within IPNs. However, this higher mRNA expression did not translate into a higher proportion of SOX9 positive cells as assessed by immunohistochemistry (**Fig. 4B** and **C**). Contrary to what we expected, aggrecan (ACAN) expression was significantly decreased in SOX9-transfected cells compared to control cells loaded within the IPNs (**Fig. 4A** and **C**), suggesting that SOX9 upregulation prior to MSC encapsulation was not suitable for inducing the expression of this ECM protein. Importantly, 2D transfection with SOX9 resulted in the downregulation of the hypertrophic marker collagen type-X at the protein level, suggesting that SOX9 transfection could be a strategy to improve the quality of the regenerated cartilage (**Fig. 4B** and **C**). Compared to soft IPNs, MSCs loaded within stiff IPNs preserve a rounded morphology at the end of the chondrogenesis experiments (**Fig. S13**), which makes it difficult to distinguish nuclear versus cytosolic staining of SOX9, and peri-cellular versus cytosolic staining of aggrecan and collagen type-X. Conversely, soft IPNs show a clear cytosolic staining for both ECM proteins, rather than extracellular. These results are consistent with diffusion limitations of the nano-porous alginate matrix, which are associated with peri-cellular matrix deposition (Loebel, Mauck, and Burdick 2019; H. P. Lee et al. 2017).

Overall, our results did not show any clear effect of stiffness in the upregulation of chondrogenic differentiation markers (Fig. 4). Accordingly, and considering the better suitability of their mechanical properties relative to loads born by articular cartilage,(Nathaniel, Mow, and Foster 1998; Hardin, Cobelli, and Santambrogio 2015) we selected the stiff 1:2 IPNs to elaborate the GAMs for the chondrogenic differentiation experiments.

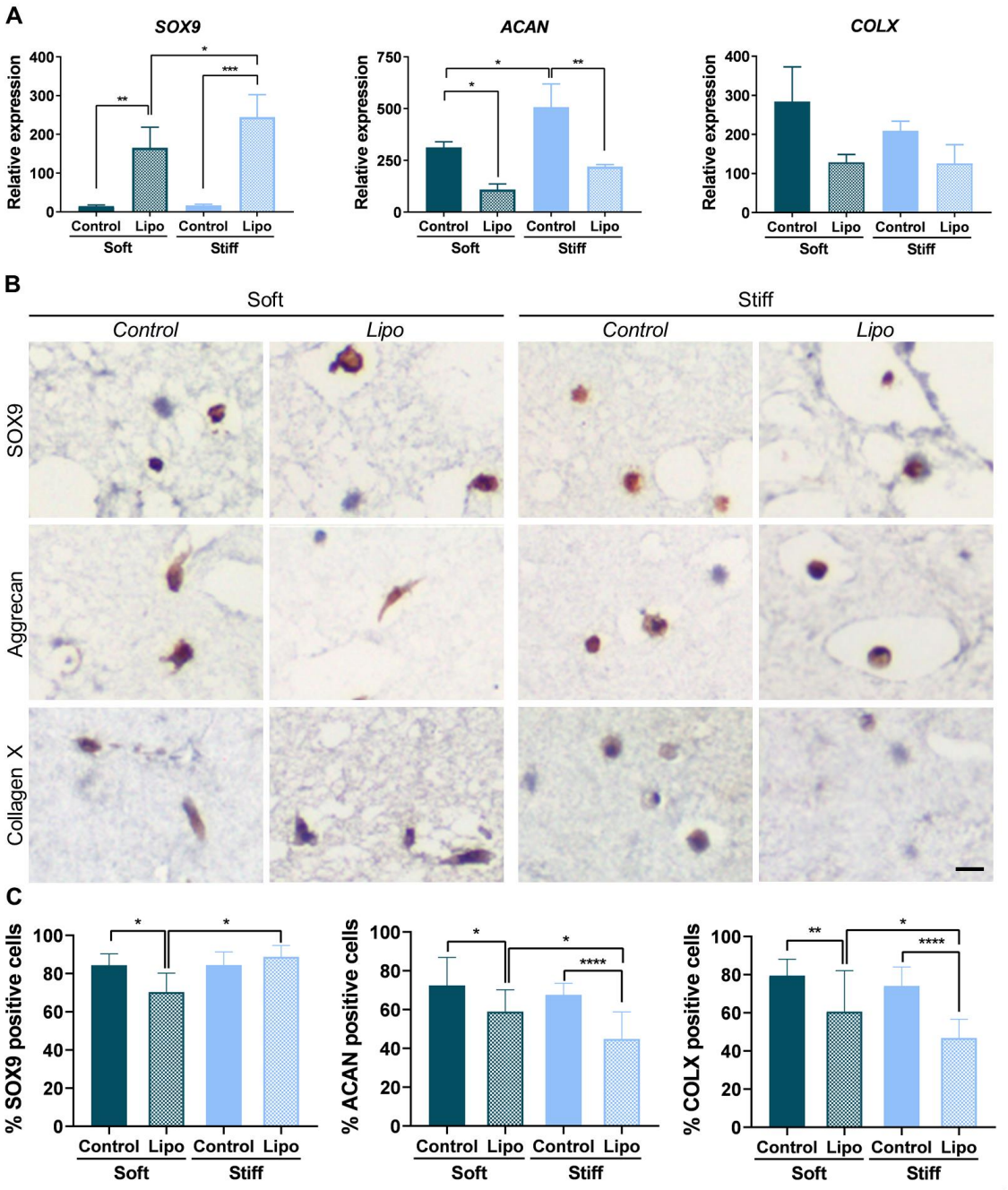

Figure 4. SOX9 2D transfection and subsequent encapsulation of adipose MSCs within the IPNs results in the reduction of collagen type-X expression. (A) Gene expression of chondrogenic markers *SOX9*, aggrecan (*ACAN*) and collagen type-X (*COLX*). Gene expression levels were measured by qRT-PCR, normalized to *GAPDH* expression and compared to the levels in MSCs before encapsulation (One-way ANOVA, *P≤0.05, **P≤0.01, ***P≤0.001, n=3). (B) Immunostaining for SOX9, aggrecan and collagen type-X in IPN sections.Scale bar = 500 µm for all the images (C) Quantification of positive cells in immunostained sections (One-way ANOVA, ****P≤0.0001, n =3). Soft designates MSCs encapsulated within soft 1:2 IPNs, Control designates MSCs encapsulated within stiff 1:2 IPNs and Lipo designates MSCs transfected with SOX9 in 2D before encapsulation within stiff 1:2 IPNs. Data represent the mean ±SD. Control and Lipo designate the IPNs loaded with non-transfected and transfected cells, respectively. See also figure S13 for lower magnification immunohistochemistry images.

We next evaluated the effect of GAM-mediated SOX9 transfection on the chondrogenic differentiation of encapsulated MSCs. First, we confirmed that SOX9-mRNA-GAMs induced a similar *SOX9* expression profile as observed for SOX9-pDNA-GAMs (**Fig. S14**). Next, adipose MSCs were loaded within stiff 1:2 GAMs (containing SOX9 mRNA nanocomplexes) and stiff 1:2 control IPNs (without nanocomplexes) and subjected to 21 days of chondrogenic differentiation, after which cells were retrieved for assessment of chondrogenic markers. As expected, SOX9-GAMs promoted a higher SOX9 gene expression than control IPNs (**Fig. 5A**). Although gene expression of chondrogenic marker aggrecan was not statistically higher compared to control IPNs, there was a significant upregulation of collagen type-II (*COL2A1*) mRNA expression in MSCs encapsulated within SOX9 GAMs (**Fig. S15**). Conversely, *COL2A1* was not detected in control IPNs. In agreement with the results obtained for the 2D transfection procedure, the levels of the hypertrophic marker collagen type-X (COLX) were lower in MSCs within SOX9-GAMs, both at the mRNA and protein level, which illustrates the role of SOX9 overexpression in controlling MSC hypertrophy (**Fig. 5A** and **C**). Importantly, no reduction in aggrecan expression was observed in MSCs loaded within SOX9 GAMs, (**Fig. 5A**), suggesting that the transfection of SOX9 within the matrices, might be more suitable to induce the expression of this chondrogenic marker as compared to the 2D transfection procedure.

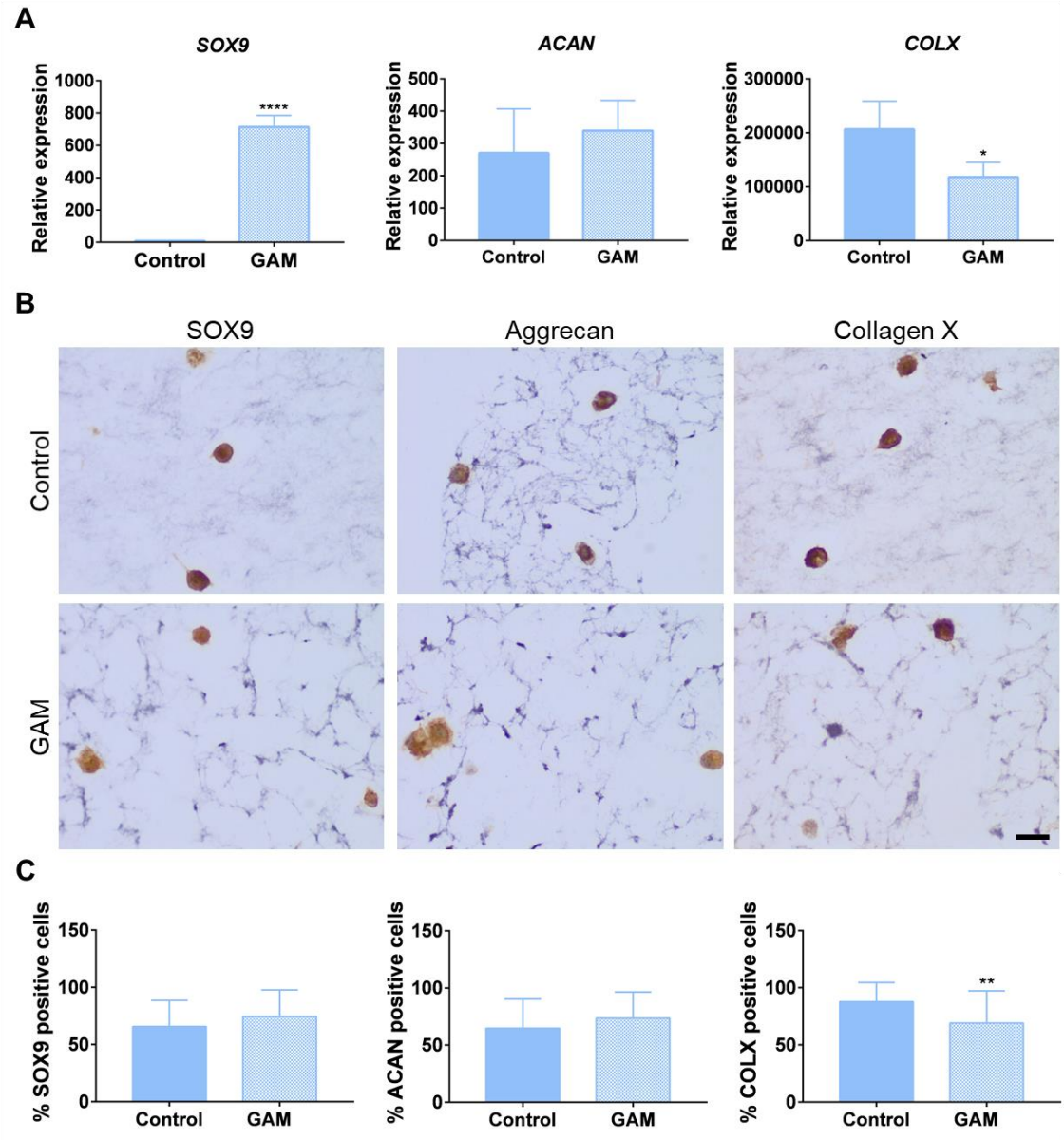

Figure 5. SOX9 3D transfection within the GAMs induces adipose MSC chondrogenic specification and reduces premature hypertrophy. (A) Gene expression of chondrogenic markers *SOX9*, aggrecan (*ACAN*) and collagen type-X (*COLX*). Gene expression levels were measured by qRT-PCR, normalized to *GAPDH* expression and compared to the levels in MSCs before encapsulation (Unpaired two-tailed t test, *P≤0.05, ****P≤0.001, n=3). (B) Immunostaining for SOX9, aggrecan and collagen type-X in GAM sections at 40x magnification. Scale bar = 20 µm for all the images. (C) Quantification of positive cells in immunostained sections (Unpaired two-tailed t test, n =3, **P≤0.01). Control designates MSCs encapsulated within IPNs and GAM designates MSCs encapsulated within IPNs loaded with SOX9 mRNA nanocomplexes (GAMs). Data represent the mean ±SD. See also Figure S15.

4. Discussion

Our data indicate that both high hydrogel stiffness and adhesion ligand densities (provided by higher collagen:alginate ratios) exert a positive effect on transgene expression. This positive effect is consistent with a similar trend observed for transfections performed in 2D and has been related to an increased cell proliferation rate(Kong et al. 2005) and a more efficient vesicular transport mediated by the

microtubular network.(Suh, Wirtz, and Hanes 2003; Dhaliwal, Oshita, and Segura 2013) In our experiments, we observed a higher gene expression of cyclin D1, a cell cycle regulator, within GAMs of higher stiffness and adhesion ligand density. In addition, our data suggest that the increased transfection efficiency of stiff GAMs is related to a higher cell uptake of the nanocomplexes. Although more studies are required to elucidate the underlying mechanism, we anticipate that the endocytic pathway and subsequent intracellular trafficking followed by the nanocomplexes are responsible for this positive effect of stiffness, based on cytoskeletal dynamics.(Dhaliwal, Oshita, and Segura 2013) These transfection results are distinct from previous reports of hyaluronic acid (HA)-based hydrogels, where soft gels induced higher cell proliferation and transgene expression levels than stiff gels.(Shiva, Talar, and Segura 2011) However, those studies tuned hydrogel stiffness with polymer concentration and utilized covalent crosslinking by Michael addition, which yields more elastic materials due to permanent covalent bonds, compared to the reversible ionic crosslinking in our system.(H. P. Lee et al. 2017)

GAM-mediated SOX9 upregulation enhanced the expression of chondrogenic markers aggrecan and collagen type-II compared to control matrices, and reduced premature production of the hypertrophic marker collagen type-X.(Dy et al. 2012) Given that the stability of mRNA inside the cell is known to be limited, particularly for non-modified sequences (Sharova et al. 2009; Tew et al. 2009; Tew and Clegg 2011), SOX9 expression at the end of the chondrogenesis experiments is mostly plausibly driven by endogenous upregulation. Indeed, this positive auto-regulation mechanism has been described in the literature (Mead et al. 2013). Additionally, it has also been described that TGF-β3 has a positive effect on the stabilization of SOX9 protein that may also contribute to this feedback loop (Coricor and Serra 2016; Chavez et al. 2017).

Contrary to what we expected, the higher SOX9 gene expression levels observed in the GAMs did not translate to a higher proportion of SOX9 positive cells compared to control matrices, as detected by immunohistochemistry. Indeed, we observed a high fraction of SOX9-positive cells in both matrices, with nearly all cell nuclei positively stained. Considering that both conditions utilized chondrogenic induction media, it is reasonable to think that this media itself,(Dahlin et al. 2014) together with the cues provided by the hydrogel,(Jiang et al. 2018) is driving a sufficient SOX9 mRNA upregulation to result in high levels of SOX9 protein expression that are difficult to discriminate by semiquantitative immunohistochemistry analysis. This might be also related to the positive auto-regulation mechanism of SOX9 mentioned previously, which may help balance the endpoint SOX9 expression in both conditions after 21 days of chondrogenic differentiation. Although endpoint SOX9 expression was similar between GAMs and control matrices, we observed a significant downregulation of the hypertrophic marker collagen type-X in GAMs compared to controls, which is consistent with previous findings (Dy et al. 2012) and points to an earlier SOX9 upregulation in the GAMs. Given the limitations of current cartilage engineering devices, the observed reduction in collagen type-X is noteworthy, because tissue engineered cartilage usually presents an inadequate balance of collagen type-II and collagen type-X, leading to a premature hypertrophic cartilage of poor mechanical properties.(Huey, Hu, and Athanasiou 2012)

Conversely, we did not observe a significant increase in aggrecan expression in the GAMs compared to the control matrices after 21 days of chondrogenesis, which may be a consequence of the similar amount of SOX9 positive cells at this time point. In this regard, it is worth mentioning that aggrecan expression was downregulated after transfection of SOX9 in 2D, as opposed to the transfection occurring within the GAM. This suggests that the direct transfection of MSCs in the 3D matrix confers an advantage

over 2D cell transfection procedures, which is particularly interesting in tissue engineering, since it allows for direct cell modification at the place of injury. Compared to previous mRNA GAMs encoding growth factors, the use of transcription factors may provide a higher potency and specificity for cell reprogramming and directed differentiation (Makiko Iwafuchi-Doi and Kenneth S. Zaret 2014; Takahashi and Yamanaka 2016; Liang et al. 2008; Graf and Enver 2009; Warren et al. 2010). Additionally, the use of mRNA has been proven more efficacious than pDNA to encode transcription factors for cell differentiation. (Warren et al. 2010; Mandal and Rossi 2013; Guo et al. 2014; Aini et al. 2016). For these reasons, and considering their biocompatibility (K. Y. Lee and Mooney 2012; Lin et al. 2019) and injectability(L. Wang et al. 2012), we believe that the IPNs described in this work are promising devices that could potentially simplify the application of cell reprogramming strategies in the clinical setting. Due to the inconsistencies in autologous stem cell populations because of donor-to-donor variability, we propose that these strategies would be better moved forward with biobanked iPSCs(Trounson and DeWitt 2016; Lui et al. 2013; Tani 2015; Kyttälä et al. 2016).

5. Conclusions

The results in this study show that matrix stiffness and cell-adhesion ligand density are key factors promoting gene delivery in collagen-I-alginate GAMs. These GAMs can be activated with SOX9 and promote MSC chondrogenesis with low hypertrophy levels, resulting in an improved chondrogenic marker expression compared to the encapsulation of 2D transfected MSCs in control matrices. These results indicate that matrix mechanics can be adjusted in order to design more efficient GAMs for in situ cell reprogramming in tissue engineering.

Acknowledgements

This work has been funded by Ministerio de Economía y Competitividad (MINECO-RETOS, Grant MAT2017-84361-R, Feder Funds), Fundación BBVA 2014-PO0110, Xunta de Galicia (Grupos de Referencia Competitiva, Feder Funds) and the National Institute of Dental and Craniofacial Research of the National Institutes of Health under Award Number R01DE013033. A. M. L. was supported by a FPU fellowship from the Spanish Ministry of Education (FPU12/05528). K. H. V. was supported by the National Institute of Dental and Craniofacial Research of the National Institutes of Health under Award Number K08DE025292. Research reported in this manuscript is solely the responsibility of the authors and does not necessarily represent the official views of the National Institutes of Health. The authors thank Thomas Ferrante for assistance with confocal reflectance microscopy, Ana Senra for assistance with immunohistochemical analysis and Dr. J. Li, Dr. S. T. Koshy and Dr. A. S. Cheung for scientific discussions.

Author contributions

Conceptualization, A.M.L., K.V., M. G. F. and D. J. M.; Methodology, A.M.L. and K.V.; Investigation, A.M.L. and K.V.; Writing – Original Draft, A.M.L. and K.V.; Writing – Review

& Editing, A.M.L., K.V., M.J.A., M.G.F. and D.J.M.; Funding Acquisition, M.G.F. and D.J.M.; Supervision, M.J.A., M.G.F. and D.J.M.

Conflict of interest

The authors declare no potential conflicts of interest with respect to the research, authorship, and/or publication of this article.

References

Aini, Hailati, Keiji Itaka, Ayano Fujisawa, Hirokuni Uchida, Satoshi Uchida, Shigeto Fukushima, Kazunori Kataoka, Taku Saito, Ung-il Chung, and Shinsuke Ohba. 2016. "Messenger RNA Delivery of a Cartilage-Anabolic Transcription Factor as a Disease-Modifying Strategy for Osteoarthritis Treatment." *Scientific Reports* 6 (November 2015). Nature Publishing Group: 18743. doi:10.1038/srep18743.

Anderson, Erin M, D Ph, Eduardo A Silva, D Ph, Yibai Hao, Kathleen D Martinick, Sarah A Lewin, Alexander G Stafford, Elisabeth G Doherty, Lin Wang, D Ph, Edward J Doherty, Paul M Grossman, Dave J Mooney, and D Ph. 2017. "VEGF and IGF Delivered from Alginate Hydrogels Promotes Stable Perfusion Recovery in Ischemic Hindlimbs of Aged Mice and Rabbits" 54 (5): 288–98. doi:10.1159/000479869.VEGF.

Balakrishnan, Biji, and R. Banerjee. 2011. "Biopolymer-Based Hydrogels for Cartilage Tissue Engineering." *Chemical Reviews* 111 (8): 4453–74. doi:10.1021/cr100123h.

Balmayor, Elizabeth R., Johannes P. Geiger, Christian Koch, Manish K. Aneja, Martijn van Griensven, Carsten Rudolph, and Christian Plank. 2016. "Modified MRNA for BMP-2 in Combination with Biomaterials Serves as a Transcript-Activated Matrix for Effectively Inducing Osteogenic Pathways in Stem Cells." *Stem Cells and Development* 26 (1): 25–34. doi:10.1089/scd.2016.0171.

Bi, Weimin, Jian Min Deng, Zhaoping Zhang, Richard R Behringer, and Benoit De Crombrugghe. 1999. "Sox9 Is Required for Cartilage Formation." *Nature Genetics* 22 (may): 85–89.

Branco da Cunha, Cristiana, Darinka D. Klumpers, Weiwei A. Li, Sandeep T. Koshy, James C. Weaver, Ovijit Chaudhuri, Pedro L. Granja, and David J. Mooney. 2014. "Influence of the Stiffness of Three-Dimensional Alginate/Collagen-I Interpenetrating Networks on Fibroblast Biology." *Biomaterials* 35 (32): 8927–36. doi:10.1016/j.biomaterials.2014.06.047.

C Hansen KC and Tyler JK, Lucia M S Das. 2017. "Substrate Stress-Relaxation Regulates Scaffold Remodeling and Bone Formation in Vivo." *Advanced Healthcare Materials* 176 (3): 139–48. doi:10.1016/j.physbeh.2017.03.040.

Chang, Tingjie, Jie Xie, Hongzhuo Li, Dong Li, Ping Liu, and Yihe Hu. 2016. "MicroRNA-30a Promotes Extracellular Matrix Degradation in Articular Cartilage via Downregulation of Sox9." *Cell Proliferation* 49 (2): 207–18. doi:10.1111/cpr.12246.

Chaudhuri, Ovijit, Luo Gu, Max Darnell, Darinka Klumpers, Sidi A. Bencherif, James C. Weaver, Nathaniel Huebsch, and David J. Mooney. 2015. "Substrate Stress Relaxation Regulates Cell Spreading." *Nature Communications* 6. Nature Publishing Group: 6365. doi:10.1038/ncomms7365.

Chaudhuri, Ovijit, Luo Gu, Darinka Klumpers, Max Darnell, Sidi A. Bencherif, James C. Weaver, Nathaniel Huebsch, Hong-pyo Lee, Evi Lippens, Georg N. Duda, and David J. Mooney. 2015. “Hydrogels with Tunable Stress Relaxation Regulate Stem Cell Fate and Activity.” *Nature Materials* 15 (3): 326–34. doi:10.1038/nmat4489.

Chaudhuri, Ovijit, Sandeep T. Koshy, Cristiana Branco Da Cunha, Jae Won Shin, Catia S. Verbeke, Kimberly H. Allison, and David J. Mooney. 2014. “Extracellular Matrix Stiffness and Composition Jointly Regulate the Induction of Malignant Phenotypes in Mammary Epithelium.” *Nature Materials* 13 (10): 970–78. doi:10.1038/nmat4009.

Chavez, R. D., G. Coricor, J. Perez, H. S. Seo, and R. Serra. 2017. “SOX9 Protein Is Stabilized by TGF-β and Regulates PAPSS2 MRNA Expression in Chondrocytes.” *Osteoarthritis and Cartilage* 25 (2). Elsevier Ltd: 332–40. doi:10.1016/j.joca.2016.10.007.

Chu, Cathy, and Hyunjoon Kong. 2012. “Interplay of Cell Adhesion Matrix Stiffness and Cell Type for Non-Viral Gene Delivery.” *Acta Biomaterialia* 8 (7). Acta Materialia Inc.: 2612–19. doi:10.1016/j.actbio.2012.04.014.

Coricor, George, and Rosa Serra. 2016. “TGF-β Regulates Phosphorylation and Stabilization of Sox9 Protein in Chondrocytes through P38 and Smad Dependent Mechanisms.” *Scientific Reports* 6 (August). Nature Publishing Group: 1–11. doi:10.1038/srep38616.

Dahlin, Rebecca L., Mengwei Ni, Ville V. Meretoja, F. Kurtis Kasper, and Antonios G. Mikos. 2014. “TGF-B3-Induced Chondrogenesis in Co-Cultures of Chondrocytes and Mesenchymal Stem Cells on Biodegradable Scaffolds.” *Biomaterials* 35 (1). Elsevier Ltd: 123–32. doi:10.1016/j.biomaterials.2013.09.086.

DeVine, John, Joseph Dettori, John France, Erika Brodt, and Robert McGuire. 2012. “The Use of RhBMP in Spine Surgery: Is There a Cancer Risk?” *Evidence-Based Spine-Care Journal* 3 (02): 35–41. doi:10.1055/s-0031-1298616.

Dhaliwal, Anandika, Maricela Maldonado, Zenas Han, and Tatiana Segura. 2010. “Differential Uptake of DNA-Poly(Ethylenimine) Polyplexes in Cells Cultured on Collagen and Fibronectin Surfaces.” *Acta Biomaterialia* 6 (9). Acta Materialia Inc.: 3436–47. doi:10.1016/j.actbio.2010.03.038.

Dhaliwal, Anandika, Victor Oshita, and Tatiana Segura. 2013. “Transfection in the Third Dimension.” *Integr Biol (Camb.)* 5 (10): 1206–16. doi:10.1038/jid.2014.371.

Dy, Peter, Weihuan Wang, Pallavi Bhattaram, Qiuqing Wang, Lai Wang, R Tracy Ballock, and Véronique Lefebvre. 2012. “Sox9 Directs Hypertrophic Maturation and Blocks Osteoblast Differentiation of Growth Plate Chondrocytes.” *Developmental Cell* 22 (3): 597–609. doi:10.1016/j.devcel.2011.12.024.

Elangovan, Satheesh, Behnoush Khorsand, Anh Vu Do, Liu Hong, Alexander Dewerth, Michael Kormann, Ryan D. Ross, D. Rick Sumner, Chantal Allamargot, and Aliasger K. Salem. 2015. “Chemically Modified RNA Activated Matrices Enhance Bone Regeneration.” *Journal of Controlled Release* 218. Elsevier B.V.: 22–28. doi:10.1016/j.jconrel.2015.09.050.

Engler, Adam J., Shamik Sen, H. Lee Sweeney, and Dennis E. Discher. 2006. “Matrix Elasticity Directs Stem Cell Lineage Specification.” *Cell* 126 (4): 677–89. doi:10.1016/j.cell.2006.06.044.

Epstein, NancyE. 2013. “Complications Due to the Use of BMP/INFUSE in Spine Surgery: The Evidence Continues to Mount.” *Surgical Neurology International* 4 (6): 343. doi:10.4103/2152-7806.114813.

Gojgini, Shiva, Talar Tokatlian, and Tatiana Segura. 2011. “Utilizing Cell-Matrix Interactions to Modulate Gene Transfer to Stem Cells inside Hyaluronic Acid Hydrogels.” *Molecular Pharmaceutics* 8 (5): 1582–91. doi:10.1021/mp200171d.

Graf, Thomas, and Tariq Enver. 2009. “Forcing Cells to Change Lineages.” *Nature* 462 (7273). Nature Publishing Group: 587–94. doi:10.1038/nature08533.

Guilak, Farshid, DM Cohen, and BT Estes. 2009. “Control of Stem Cell Fate by Physical Interactions with the Extracellular Matrix.” *Cell Stem Cell* 5 (1): 17–26. doi:10.1016/j.stem.2009.06.016.Control.

Guo, Xing Rong, Xiao Li Wang, Man Chol Li, Ya Hong Yuan, Yun Chen, Dan Dan Zou, Liu Jiao Bian, and Dong Sheng Li. 2014. “PDX-1 MRNA-Induced Reprogramming of Mouse Pancreas-Derived Mesenchymal Stem Cells into Insulin-Producing Cells in Vitro.” *Clinical and Experimental Medicine* 15 (4): 501–9. doi:10.1007/s10238-014-0319-0.

Hardin, John A., Neil Cobelli, and Laura Santambrogio. 2015. “Consequences of Metabolic and Oxidative Modifications of Cartilage Tissue.” *Nature Reviews Rheumatology* 11 (9). Nature Publishing Group: 521–29. doi:10.1038/nrrheum.2015.70.

Hinderer, Svenja, Shannon Lee Layland, and Katja Schenke-Layland. 2016. “ECM and ECM-like Materials - Biomaterials for Applications in Regenerative Medicine and Cancer Therapy.” *Advanced Drug Delivery Reviews* 97. The Authors: 260–69. doi:10.1016/j.addr.2015.11.019.

Holcik, M, and S a Liebhaber. 1997. “Four Highly Stable Eukaryotic MRNAs Assemble 3’ Untranslated Region RNA-Protein Complexes Sharing Cis and Trans Components.” *Proceedings of the National Academy of Sciences of the United States of America* 94 (6): 2410–14. doi:10.1073/pnas.94.6.2410.

Huebsch, Nathaniel, Praveen R. Arany, Angelo S. Mao, Dmitry Shvartsman, Omar A. Ali, Sidi A. Bencherif, José Rivera-Feliciano, and David J. Mooney. 2010. “Harnessing Traction-Mediated Manipulation of the Cell/Matrix Interface to Control Stem-Cell Fate.” *Nature Materials* 9 (6). Nature Publishing Group: 518–26. doi:10.1038/nmat2732.

Huey, Daniel J., Jerry C. Hu, and Kyriacos A. Athanasiou. 2012. “Unlike Bone, Cartilage Regeneration Remains Elusive.” *Science* 338 (6109): 917–21. doi:10.1126/science.1222454.

Im, Gun I., Hye Joung Kim, and Jin H. Lee. 2011. “Chondrogenesis of Adipose Stem Cells in a Porous PLGA Scaffold Impregnated with Plasmid DNA Containing SOX Trio (SOX-5,-6 and -9) Genes.” *Biomaterials* 32 (19). Elsevier Ltd: 4385–92. doi:10.1016/j.biomaterials.2011.02.054.

Jiang, Xianfang, Xianyuan Huang, Tongmeng Jiang, Li Zheng, Jinmin Zhao, and Xingdong Zhang. 2018. “The Role of Sox9 in Collagen Hydrogel-Mediated Chondrogenic Differentiation of Adult Mesenchymal Stem Cells (MSCs).” *Biomaterials Science* 6 (6). Royal Society of Chemistry: 1556–68. doi:10.1039/c8bm00317c.

Jopling, Chris, Stephanie Boue, and Juan Carlos Izpisua Belmonte. 2011. “Dedifferentiation, Transdifferentiation and Reprogramming: Three Routes to Regeneration.” *Nature Reviews Molecular Cell Biology* 12 (2). Nature Publishing Group: 79–89. doi:10.1038/nrm3043.

Kang, Daniel G., Wellington K. Hsu, and Ronald A. Lehman. 2017. “Complications

Associated With Bone Morphogenetic Protein in the Lumbar Spine." *Orthopedics* 40 (2): e229–37. doi:10.3928/01477447-20161213-06.

Khorsand, Behnoush, Satheesh Elangovan, Liu Hong, Alexander Dewerth, Michael S. D. Kormann, and Aliasger K. Salem. 2017. "A Comparative Study of the Bone Regenerative Effect of Chemically Modified RNA Encoding BMP-2 or BMP-9." *The AAPS Journal* 19 (2). The AAPS Journal: 438–46. doi:10.1208/s12248-016-0034-8.

Kong, Hyun Joon, Jodi Liu, Kathryn Riddle, Takuya Matsumoto, Kent Leach, and David J. Mooney. 2005. "Non-Viral Gene Delivery Regulated by Stiffness of Cell Adhesion Substrates." *Nature Materials* 4 (6): 460–64. doi:10.1038/nmat1392.

Kozak, Marilyn. 1987. "An Analysis of 5'-Noncoding Sequences from 699 Vertebrate Messenger RNAS." *Nucleic Acids Research* 15 (20): 8125–48. doi:10.1093/nar/15.20.8125.

Kyttälä, Aija, Roksana Moraghebi, Cristina Valensisi, Johannes Kettunen, Colin Andrus, Kalyan Kumar Pasumarthy, Mahito Nakanishi, Ken Nishimura, Manami Ohtaka, Jere Weltner, Ben Van Handel, Olavi Parkkonen, Juha Sinisalo, Anu Jalanko, R. David Hawkins, Niels Bjarne Woods, Timo Otonkoski, and Ras Trokovic. 2016. "Genetic Variability Overrides the Impact of Parental Cell Type and Determines IPSC Differentiation Potential." *Stem Cell Reports* 6 (2): 200–212. doi:10.1016/j.stemcr.2015.12.009.

Lee, Hong Pyo, Luo Gu, David J. Mooney, Marc E. Levenston, and Ovijit Chaudhuri. 2017. "Mechanical Confinement Regulates Cartilage Matrix Formation by Chondrocytes." *Nature Materials* 16 (12): 1243–51. doi:10.1038/nmat4993.

Lee, Kuen Yong, and David J. Mooney. 2012. "Alginate: Properties and Biomedical Applications." *Progress in Polymer Science (Oxford)* 37 (1): 106–26. doi:10.1016/j.progpolymsci.2011.06.003.

Lei, Pedro, Roshan M. Padmashali, and Stelios T. Andreadis. 2009. "Cell-Controlled and Spatially Arrayed Gene Delivery from Fibrin Hydrogels." *Biomaterials* 30 (22). Elsevier Ltd: 3790–99. doi:10.1016/j.biomaterials.2009.03.049.

Liang, Qing Le, Xiao Xun Wang, Xiao Fei Yan, Li Jun Yang, Dong Qi Tang, and Dong Sheng Li. 2008. "Transcription Factor Directed Differentiation of Human Embryonic Stem Cells into the Pancreatic Endocrine Lineage." *Cell Research* 18: S109–S109. doi:10.1038/cr.2008.199.

Lin, Kaili, Dawei Zhang, Maria Helena Macedo, Wenguo Cui, Bruno Sarmento, and Guofang Shen. 2019. "Advanced Collagen-Based Biomaterials for Regenerative Biomedicine." *Advanced Functional Materials* 29 (3): 1–16. doi:10.1002/adfm.201804943.

Lo, Kevin W-H, Bret D Ulery, Keshia M Ashe, and Cato T Laurencin. 2012. "Studies of Bone Morphogenetic Protein-Based Surgical Repair." *Advanced Drug Delivery Reviews* 64 (12): 1277–91. doi:10.1016/j.addr.2012.03.014.

Loebel, Claudia, Robert L. Mauck, and Jason A. Burdick. 2019. "Local Nascent Protein Deposition and Remodelling Guide Mesenchymal Stromal Cell Mechanosensing and Fate in Three-Dimensional Hydrogels." *Nature Materials* 18 (8). Springer US: 883–91. doi:10.1038/s41563-019-0307-6.

Lui, Kathy O., Lior Zangi, Eduardo A. Silva, Lei Bu, Makoto Sahara, Ronald A. Li, David J. Mooney, and Kenneth R. Chien. 2013. "Driving Vascular Endothelial Cell Fate of Human Multipotent Isl1 + Heart Progenitors with VEGF Modified MRNA." *Cell*

Research 23 (10). Nature Publishing Group: 1172–86. doi:10.1038/cr.2013.112.

Makiko Iwafuchi-Doi and Kenneth S. Zaret. 2014. “Pioneer Transcription Factors in Cell Reprogramming.” *Genes and Development* 28 (May): 2679–92. doi:10.1210/me.2014-1084.

Mandal, Pankaj K, and Derrick J Rossi. 2013. “Reprogramming Human Fibroblasts to Pluripotency Using Modified MRNA.” *Nature Protocols* 8 (3): 568–82. doi:10.1038/nprot.2013.019.

Martinez-Sanchez, Aida, and Chris L. Murphy. 2013. “MiR-1247 Functions by Targeting Cartilage Transcription Factor SOX9.” *Journal of Biological Chemistry* 288 (43): 30802–14. doi:10.1074/jbc.M113.496729.

Mead, Timothy J, Qiuqing Wang, Pallavi Bhattaram, Peter Dy, and Solomon Afelik. 2013. “A Far-Upstream (-70 Kb) Enhancer Mediates Sox9 Auto-Regulation in Somatic Tissues during Development and Adult Regeneration.” *Nucleic Acids Research* 41 (8): 4459–69. doi:10.1093/nar/gkt140.

Merrell, Allyson J., and Ben Z. Stanger. 2016. “Adult Cell Plasticity in Vivo: De-Differentiation and Transdifferentiation Are Back in Style.” *Nature Reviews Molecular Cell Biology* 17 (7). Nature Publishing Group: 413–25. doi:10.1038/nrm.2016.24.

Mirzamohammadi, Fatemeh, Garyfallia Papaioannou, and Tatsuya Kobayashi. 2014. “MicroRNAs in Cartilage Development, Homeostasis, and Disease.” *Current Osteoporosis Reports* 12 (4): 410–19. doi:10.1007/s11914-014-0229-9.

Murry, Charles E., and Gordon Keller. 2008. “Differentiation of Embryonic Stem Cells to Clinically Relevant Populations: Lessons from Embryonic Development.” *Cell* 132 (4): 661–80. doi:10.1016/j.cell.2008.02.008.

Nakamura, Yukio, Xinjun He, Hiroyuki Kato, Shigeyuki Wakitani, Tatsuya Kobayashi, Sumiko Watanabe, Atsumi Iida, Hideaki Tahara, Matthew L. Warman, Ramida Watanapokasin, and John H. Postlethwait. 2012. “Sox9 Is Upstream of MicroRNA-140 in Cartilage.” *Applied Biochemistry and Biotechnology* 166 (1): 64–71. doi:10.1007/s12010-011-9404-y.

Nathaniel, P, Van C Mow, and Robert J Foster. 1998. “Composition and Dynamics of Articular Cartilage : Structure, Function, and Maintaining a Healthy State.” *Journal of Ortophaedic & Sports Physical Therapy* 28 (4): 203–15.

Perlstein, I., J. M. Connolly, X. Cui, C. Song, Q. Li, P. L. Jones, Z. Lu, S. DeFelice, B. Klugherz, R. Wilensky, and R. J. Levy. 2003. “DNA Delivery from an Intravascular Stent with a Denatured Collagen-Polylactic-Polyglycolic Acid-Controlled Release Coating: Mechanisms of Enhanced Transfection.” *Gene Therapy* 10 (17): 1420–28. doi:10.1038/sj.gt.3302043.

Pfaffl, M. W. 2001. “A New Mathematical Model for Relative Quantification in Real-Time RT-PCR.” *Nucleic Acids Research* 29 (9): 45e – 45. doi:10.1093/nar/29.9.e45.

Raisin, Sophie, Emmanuel Belamie, and Marie Morille. 2016. “Non-Viral Gene Activated Matrices for Mesenchymal Stem Cells Based Tissue Engineering of Bone and Cartilage.” *Biomaterials* 104. Elsevier Ltd: 223–37. doi:10.1016/j.biomaterials.2016.07.017.

Sahin, Ugur, Katalin Karikó, and Özlem Türeci. 2014. “MRNA-Based Therapeutics — Developing a New Class of Drugs.” *Nature Reviews Drug Discovery* 13 (10). Nature Publishing Group: 759–80. doi:10.1038/nrd4278.

Schindelin, Johannes, Ignacio Arganda-Carreras, Erwin Frise, Verena Kaynig, Mark Longair, Tobias Pietzsch, Stephan Preibisch, Curtis Rueden, Stephan Saalfeld, Benjamin Schmid, Jean Yves Tinevez, Daniel James White, Volker Hartenstein, Kevin Eliceiri, Pavel Tomancak, and Albert Cardona. 2012. “Fiji: An Open-Source Platform for Biological-Image Analysis.” *Nature Methods* 9 (7): 676–82. doi:10.1038/nmeth.2019.

Sharova, Lioudmila V., Alexei A. Sharov, Timur Nedorezov, Yulan Piao, Nabeebi Shaik, and Minoru S H Ko. 2009. “Database for MRNA Half-Life of 19 977 Genes Obtained by DNA Microarray Analysis of Pluripotent and Differentiating Mouse Embryonic Stem Cells.” *DNA Research* 16 (1): 45–58. doi:10.1093/dnares/dsn030.

Shepard, Jaclyn A., Alyssa Huang, Ariella Shikanov, and Lonnie D. Shea. 2010. “Balancing Cell Migration with Matrix Degradation Enhances Gene Delivery to Cells Cultured Three-Dimensionally within Hydrogels.” *Journal of Controlled Release*. doi:10.1016/j.jconrel.2010.04.032.

Shiva, Gojgini, Tokatlian Talar, and Tatiana Segura. 2011. “Utilizing Cell-Matrix Interactions to Modulate Gene Transfer to Stem Cells Inside Hyaluronic Acid Hydrogels.” *Molecular Pharmaceutics* 8 (5): 1582–91. doi:10.1016/j.humov.2008.02.015.Changes.

Suh, J., D. Wirtz, and J. Hanes. 2003. “Efficient Active Transport of Gene Nanocarriers to the Cell Nucleus.” *Proceedings of the National Academy of Sciences* 100 (7): 3878–82. doi:10.1073/pnas.0636277100.

Takahashi, Kazutoshi, and Shinya Yamanaka. 2016. “A Decade of Transcription Factor-Mediated Reprogramming to Pluripotency.” *Nature Reviews Molecular Cell Biology* 17 (3). Nature Publishing Group: 183–93. doi:10.1038/nrm.2016.8.

Tani, Kenzaburo. 2015. “Towards the Safer Clinical Translation of Human Induced Pluripotent Stem Cell–Derived Cells to Regenerative Medicine.” *Molecular Therapy - Methods and Clinical Development* 2. Official journal of the American Society of Gene & Cell Therapy: 15032. doi:10.1038/mtm.2015.32.

Tew, Simon R., and Peter D. Clegg. 2011. “Analysis of Post Transcriptional Regulation of SOX9 MRNA during in Vitro Chondrogenesis.” *Tissue Engineering - Part A* 17 (13–14): 1801–7. doi:10.1089/ten.tea.2010.0579.

Tew, Simon R., Mandy J. Peffers, Tristan R. McKay, Emma T. Lowe, Wasim S. Khan, Timothy E. Hardingham, and Peter D. Clegg. 2009. “Hyperosmolarity Regulates SOX9 MRNA Posttranscriptionally in Human Articular Chondrocytes.” *American Journal of Physiology - Cell Physiology* 297 (4): 898–906. doi:10.1152/ajpcell.00571.2008.

Trounson, Alan, and Natalie D. DeWitt. 2016. “Pluripotent Stem Cells Progressing to the Clinic.” *Nature Reviews Molecular Cell Biology* 17 (3). Nature Publishing Group: 194–200. doi:10.1038/nrm.2016.10.

Vining, Kyle H., and David J. Mooney. 2017. “Mechanical Forces Direct Stem Cell Behaviour in Development and Regeneration.” *Nature Reviews Molecular Cell Biology* 18 (12). Nature Publishing Group: 728–42. doi:10.1038/nrm.2017.108.

Wang, Dan, Phillip W.L. Tai, and Guangping Gao. 2019. “Adeno-Associated Virus Vector as a Platform for Gene Therapy Delivery.” *Nature Reviews Drug Discovery* 18 (5). Springer US: 358–78. doi:10.1038/s41573-019-0012-9.

Wang, Ying A, Xiong Yu, Philip M Silverman, Robin L Harris, and H Edward. 2007. “Nanoscale Cell Adhesion Ligand Presentation Regulates Non- Viral Gene Delivery

and Expression Hyun." *Nano Letters* 7 (1): 161–66. doi:10.1016/j.jmb.2008.10.054.The.

Warren, Luigi, Philip D. Manos, Tim Ahfeldt, Yuin Han Loh, Hu Li, Frank Lau, Wataru Ebina, Pankaj K. Mandal, Zachary D. Smith, Alexander Meissner, George Q. Daley, Andrew S. Brack, James J. Collins, Chad Cowan, Thorsten M. Schlaeger, and Derrick J. Rossi. 2010. "Highly Efficient Reprogramming to Pluripotency and Directed Differentiation of Human Cells with Synthetic Modified MRNA." *Cell Stem Cell* 7 (5): 618–30. doi:10.1016/j.stem.2010.08.012.

Yamamizu, Kohei, Yulan Piao, Alexei A. Sharov, Veronika Zsiros, Hong Yu, Kazu Nakazawa, David Schlessinger, and Minoru S.H. Ko. 2013. "Identification of Transcription Factors for Lineage-Specific ESC Differentiation." *Stem Cell Reports* 1 (6). Elsevier: 545–59. doi:10.1016/j.stemcr.2013.10.006.

Yannas, I V, E Lee, D P Orgill, E M Skrabut, and G F Murphy. 1989. "Synthesis and Characterization of a Model Extracellular Matrix That Induces Partial Regeneration of Adult Mammalian Skin." *Proceedings of the National Academy of Sciences of the United States of America* 86 (3): 933–37. doi:10.1073/pnas.86.3.933.

Zhang, Haiyuan, Moo-yeal Lee, Michael G Hogg, Jonathan S Dordick, and Susan T Sharfstein. 2010. "Gene Delivery in Three-Dimensional Nanoparticles." *ACS Nano* 4 (8): 4733–43.

Zhang, Haiyuan, Moo Yeal Lee, Michael G. Hogg, Jonathan S. Dordick, and Susan T. Sharfstein. 2012. "High-Throughput Transfection of Interfering RNA into a 3D Cell-Culture Chip." *Small* 8 (13): 2091–98. doi:10.1002/smll.201102205.

SUPPORTING INFORMATION

Supplementary methods

2D Lipofectamine® 2000 transfection

For 2D transfections, cells were plated in 96 well plates approximately 12 h prior to transfection at a density of 90000 (U87MG) or 75000 (hMSCs) cells/cm^2. Four hours before transfection, media was changed to OptiMEM reduced serum medium (Gibco). For transfections performed in the presence of alginate and $CaCl_2$, both compounds were diluted in OptiMEM at the desired final concentrations and added to the cells immediately before transfection. Then, 50 µl of Lipofectamine complexes (Gibco), at 0.5:1 Lipofectamine:DNA/RNA ratios (µl:µg), were prepared in OptiMEM following manufacturer's instructions. Briefly, a solution containing 1 µg of mRNA/pDNA was added over a solution containing 0.5 µl of Lipofectamine® 2000 reagent in a 1/1 v/v ratio, mixed by pipetting up-down and incubated for 20 min at room temperature. Complexes were added over the cells drop-by-drop and incubated for 6 hours. Subsequently, complexes were aspirated and cells were maintained in regular growing media until analysis. The transfection reaction was escalated for plates of higher surface areas.

Supporting figures

Table S1. List of TaqMan® assays employed for qRT-PCR experiments.

TaqMan assays (Applied Biosystems)	
SOX9 (human)	Hs00165814_m1
ACAN (human)	Hs 00153936_m1
COL2A1 (human)	Hs00264051_m1
COL10A1 (human)	Hs00166657_m1
ACT B (human)	Hs99999903_m1
GAPDH (human)	Hs99999905_m1

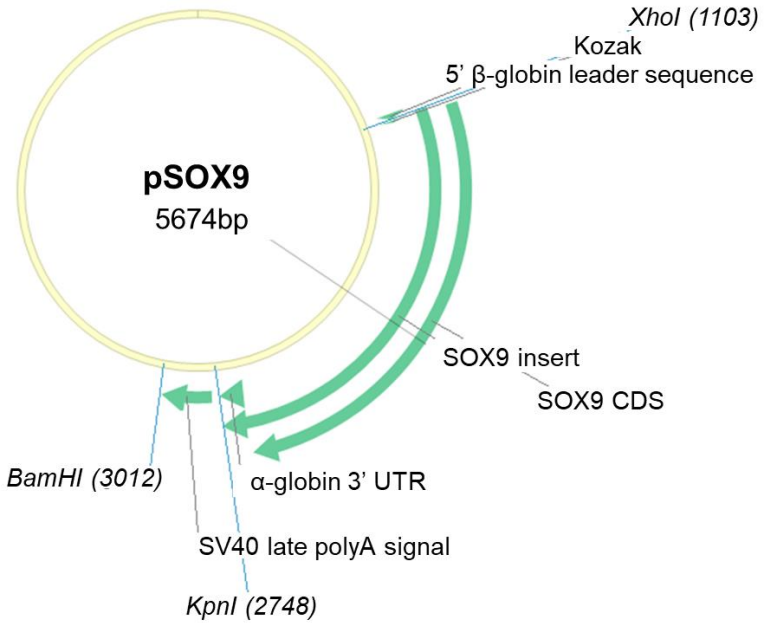

Figure S1. SOX9 plasmid used as template for SOX9 mRNA synthesis. Map shows the SOX9 coding sequence (CDS) and relevant restriction sites.

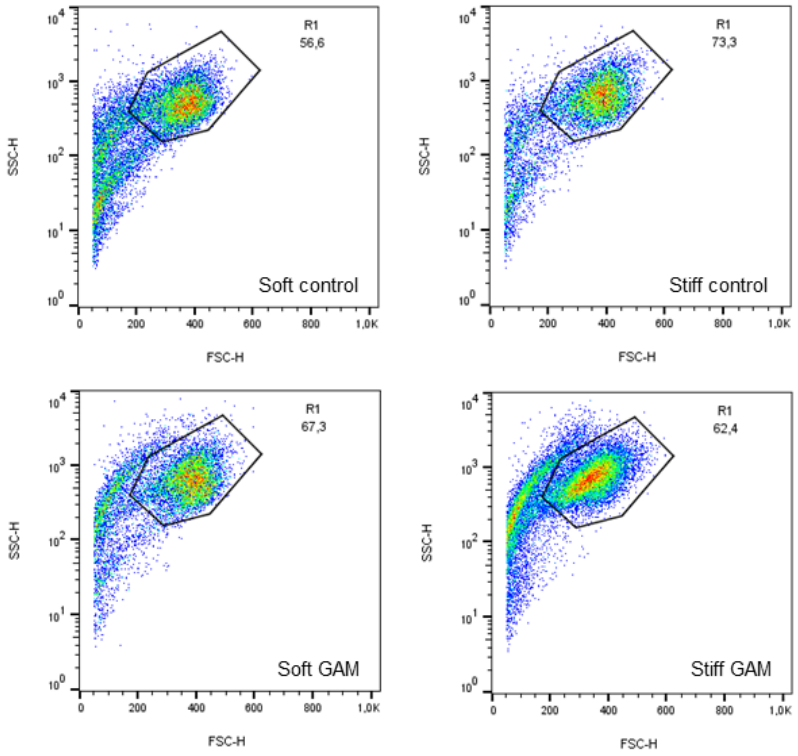

Figure S2. Gating scheme for the evaluation of Cy5-pDNA association to MSCs. Soft control and stiff control designate the cells recovered from the blank IPNs (no nanocomplexes). Soft GAM and stiff GAM designate the cells recovered from the IPNs loaded with the nanocomplexes (GAMs).

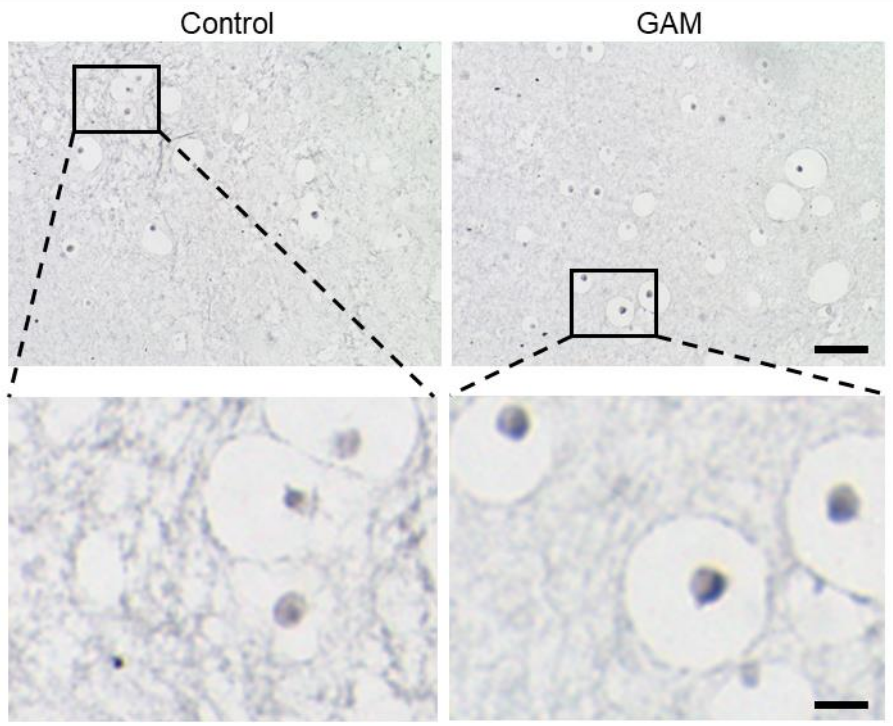

Figure S3. Negative controls in immunohistochemistry sections obtained from Stiff 1:2 IPNs by omitting the primary antibodies. Scale bars = 100 µm and 500 µm for the original images and image insets, respectively.

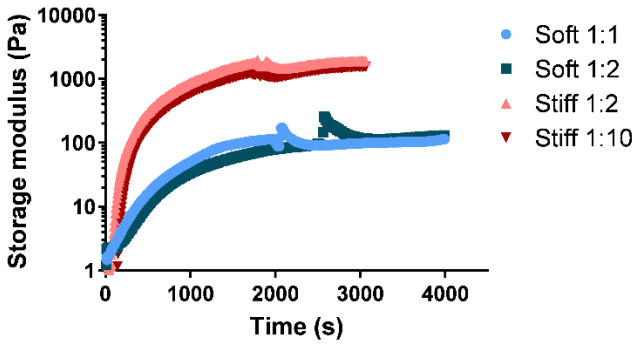

Figure S4. Evolution of the storage modulus with time. Storage modulus at 0.5% strain and 1 Hz was recorded periodically until it reached its equilibrium value. Curve inflections reflect the change in temperature to 37°C for collagen crosslinking, and the addition of HBSS to avoid IPN dehydration. Data is representative of at least three measurements for each condition.

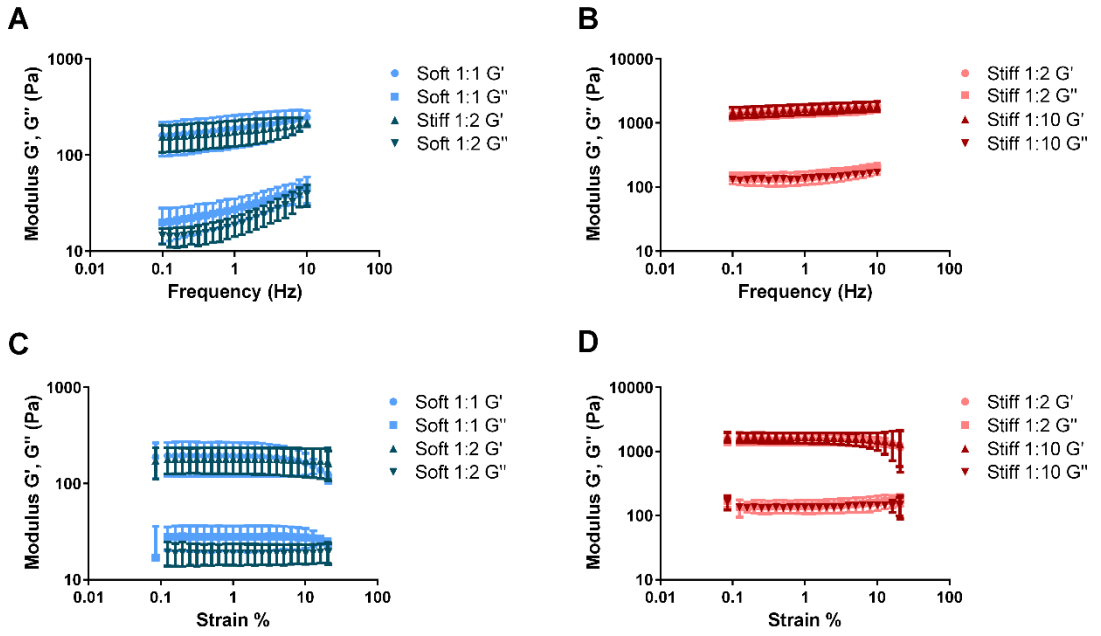

Figure S5. Strain and frequency sweeps of the IPN set. Frequency dependent rheology of soft (A) and stiff (B) IPNs performed at 1% strain after gelation was completed. Strain sweep (1 Hz) of soft (D) and stiff (D) IPNs. Data represent the mean ±SD.

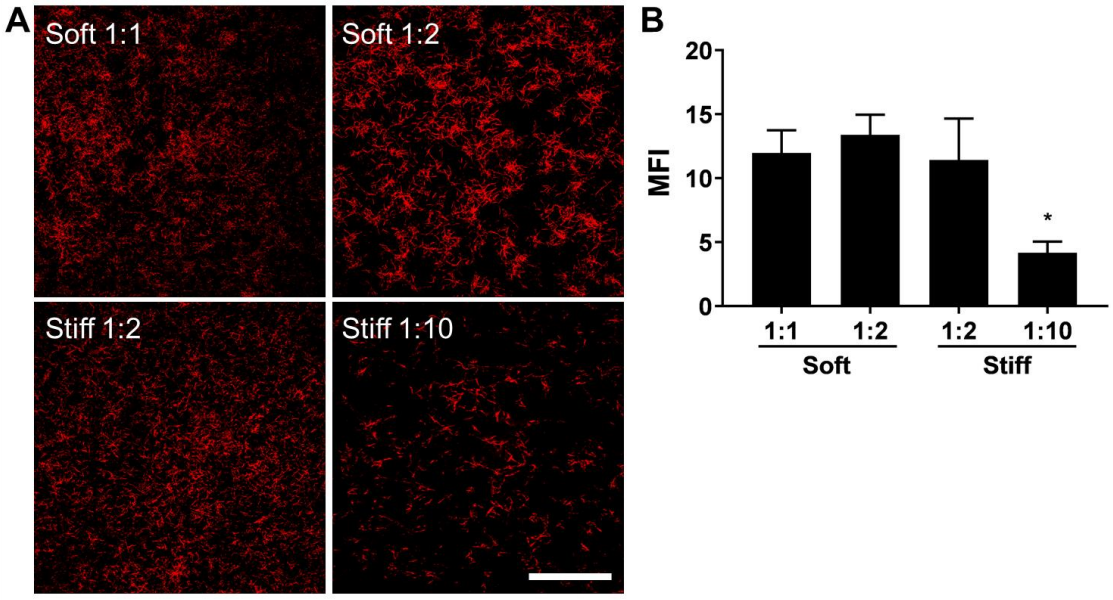

Figure S6. Amount and distribution of collagen fibers within the IPN set. Collagen fiber alignment as assessed by confocal reflectance microscopy. Scale bar = 100 µm for all the images (A). Mean fluorescence intensity (MFI) quantification of A) (B). One-way ANOVA was performed to compare MFI levels (*P≤0.05).

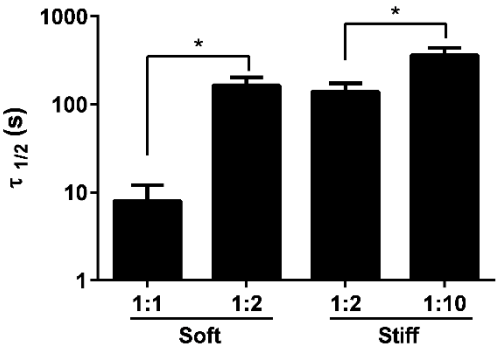

Figure S7. Quantification of timescale at which the stress is relaxed to half its original value, τ1/2, in stress-relaxation tests (shear stress 15% in 1 s) (One-way ANOVA, n=3, *P<0.05).

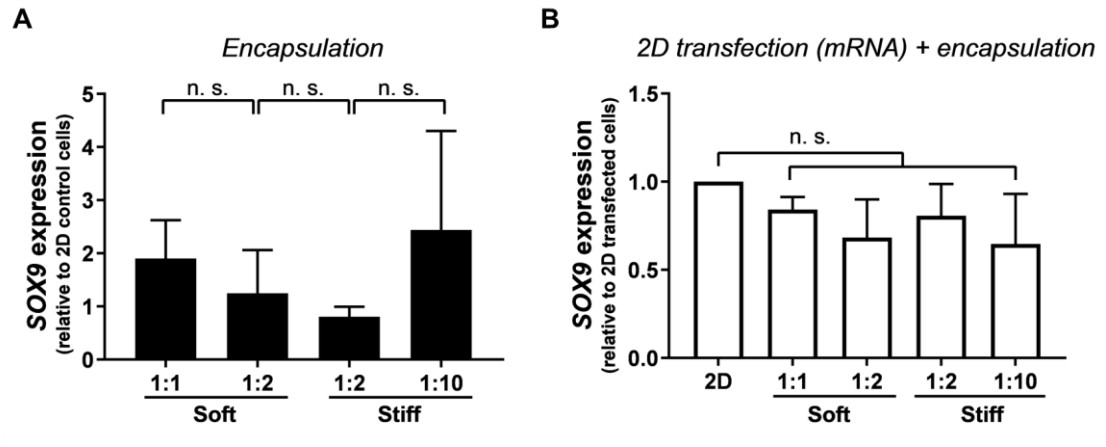

Figure S8. *SOX9* expression after encapsulation of control bMSCs or 2D mRNA transfected bMSCs within blank IPNs. *SOX9* expression 48 h after encapsulation of control (non-transfected) bMSCs (A). SOX9 expression 24 h after encapsulation of bMSCs transfected with SOX9 mRNA in 2D (B). Gene expression levels were normalized to GAPDH and compared to the levels in transfected bMSCs before encapsulation. One-way ANOVA with a Tukey's post-hoc multiple comparison test was performed to compare gene expression levels between the IPNs (A) or the IPNs and transfected bMSCs before encapsulation (B). IPNs are described by their stiffness and collagen:alginate w:w ratios (1:1 to 1:10).

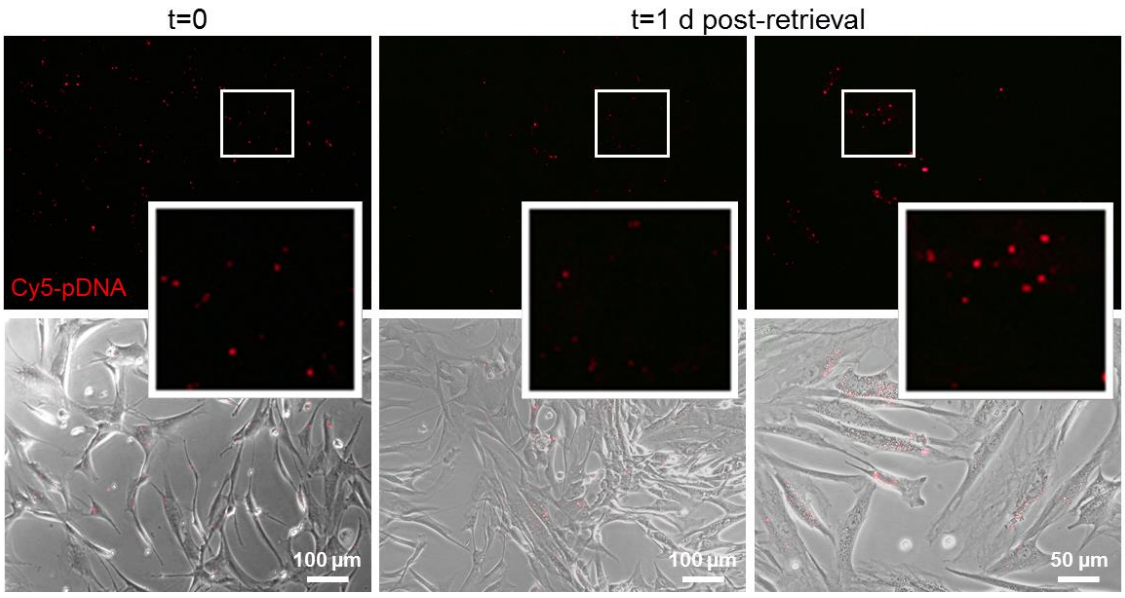

Figure S9. Location of Cy5-labeled pDNA complexes in cells retrieved from tissue culture plates after 2D pDNA transfection. Transfection complexes were incubated with hMSCs for 4 h and media was changed afterwards (t=0). Cells were cultured for 72 h and then retrieved by enzymatic separation and transferred to a new plate. Images were taken one day after retrieval (t=1 d post-retrieval).

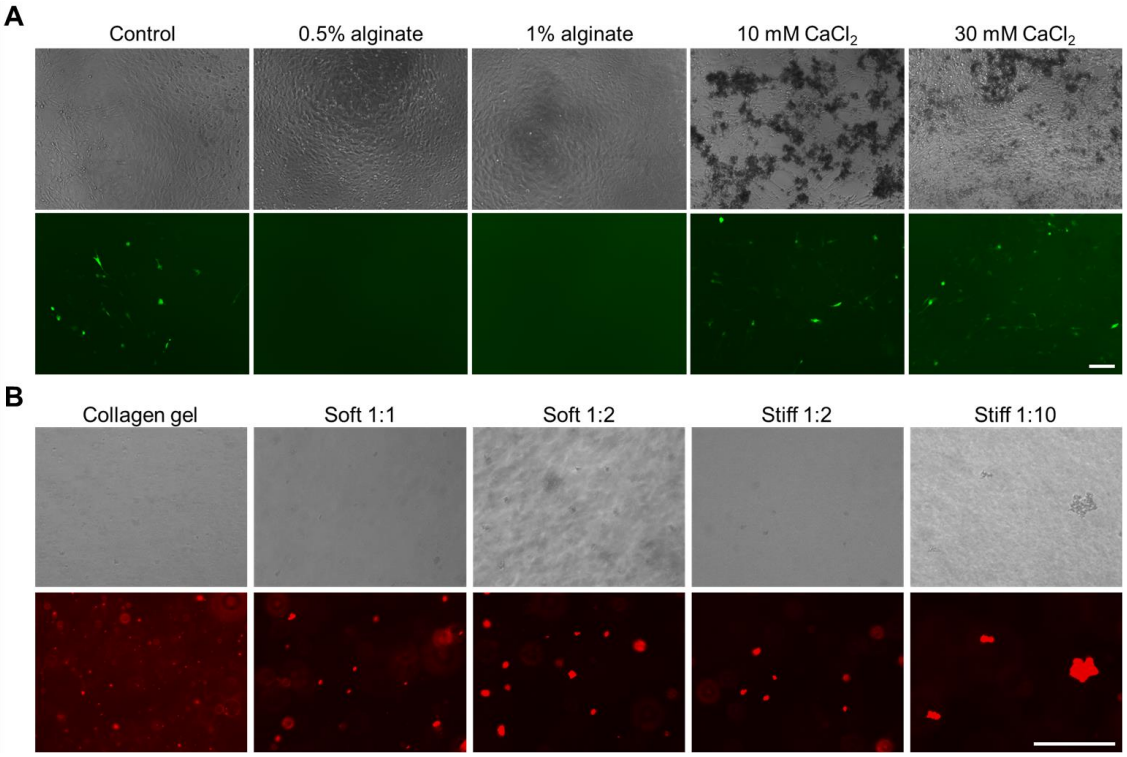

Figure S10. Alginate impairs 2D transfection and promotes the aggregation of the pDNA condensates within the IPNs. (A) Effect of alginate and $CaCl_2$ on 2D transfection. Fluorescence micrographs of 3T3 fibroblasts 72 h after YFP pDNA transfection with Lipofectamine® 2000 lipoplexes in the presence of increasing alginate and $CaCl_2$ concentrations compared to control (transfection in culture media). Scale bar = 100 µm for all the images. (B) Distribution of labeled pDNA 3DFectIN® complexes within the IPNs and a control 0.5% w/v collagen gel. Optical (top) and fluorescence (bottom) micrographs. Scale bar = 200 µm for all the images.

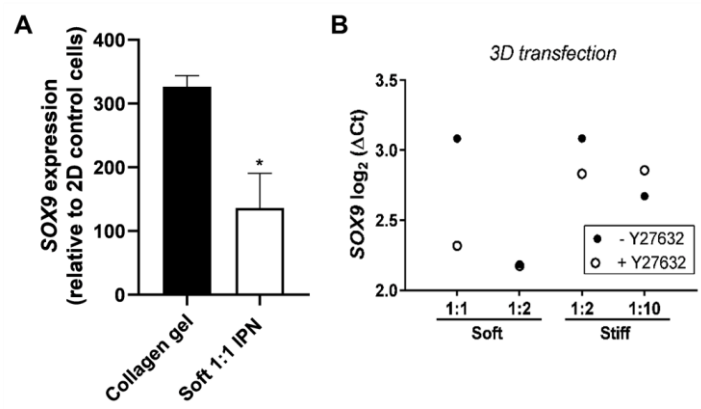

Figure S11. Effect of collagen and ROCK inhibition on GAM transfection efficiency. hMSCs were transfected with SOX9 pDNA within a 0.5% collagen gel or soft 1:1 IPN (Unpaired two tailed t-test, *P≤0.05, n=2) (A). hMSCs were transfected with SOX9 pDNA within the IPNs in the absence or presence of Y-27632 (B). For soft 1:2 IPNs, SOX9 expression was very similar with and without the ROCK inhibitor and only the Y-27632 point is visible.

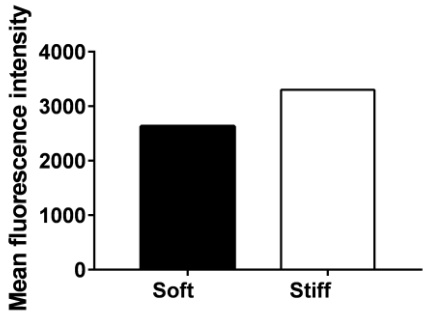

Figure S12. Flow cytometry analysis of the Mean Fluorescence Intensity of MSCs encapsulated within soft and stiff GAMs loaded with Cy5-labeled pDNA.

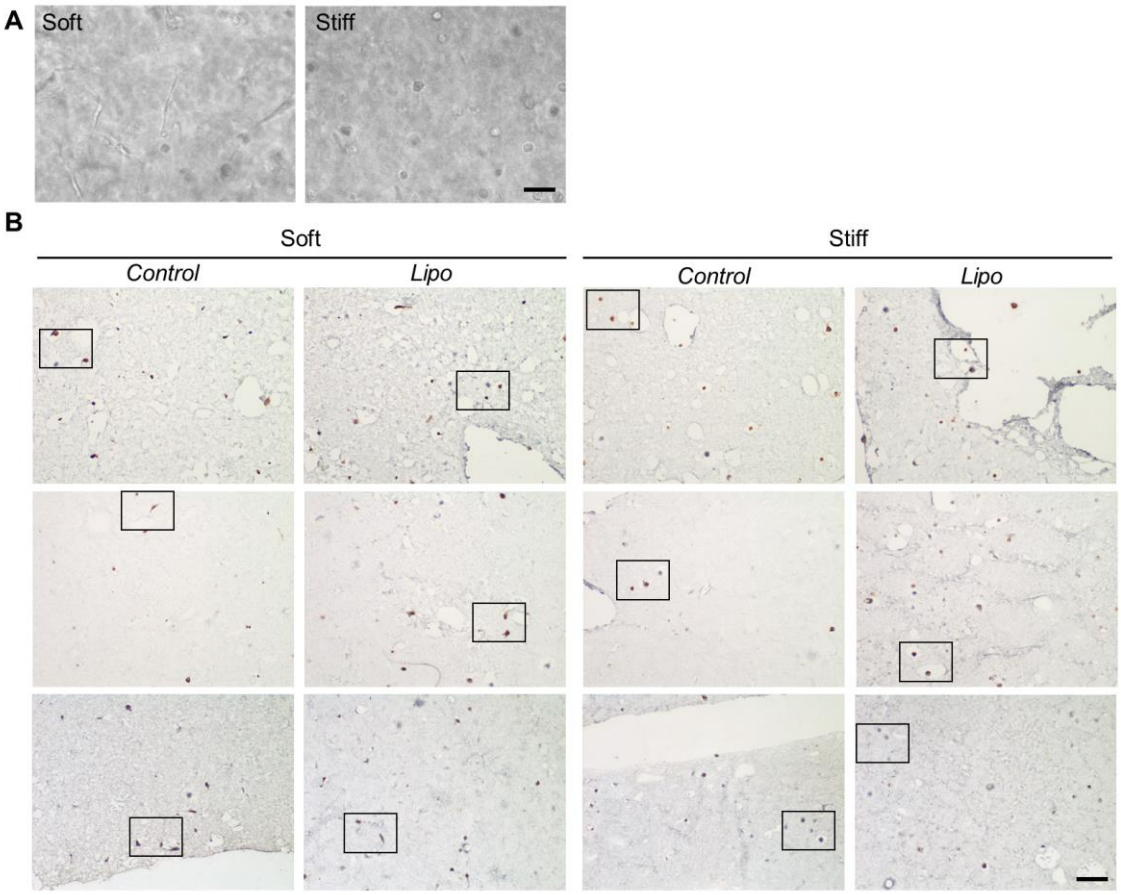

Figure S13. Immunostaining of soft and stiff IPNs after 2D *SOX9* transfection. Bright field image of adipose MSCs loaded within soft and stiff IPNs after 21 days of chondrogenic induction (A). Scale bar = 50 µm for all the images. Lower magnification images of the immunostaining sections of SOX9, aggrecan and collagen type-X shown in Figure 4, indicating the location of the insets shown (B). Scale bar = 100 µm for all the images.

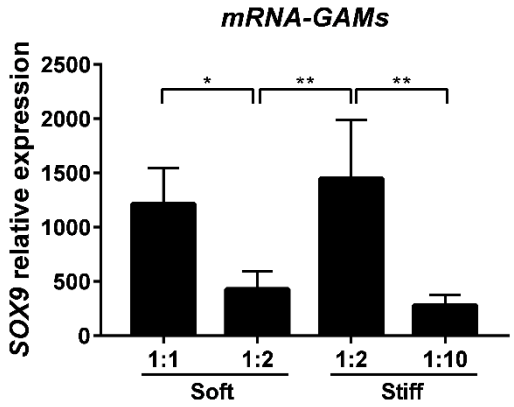

Figure S14. *SOX9* expression 24 h after bMSC encapsulation within mRNA-GAMs. Gene expression levels were measured by qRT-PCR, normalized to *GAPDH* expression and compared to the levels in bMSCs before encapsulation. One-way ANOVA was performed to compare gene expression levels (**P≤0.01; ***P≤0.001; ****P≤0.0001) (n=3). Data represent the mean ± SD.

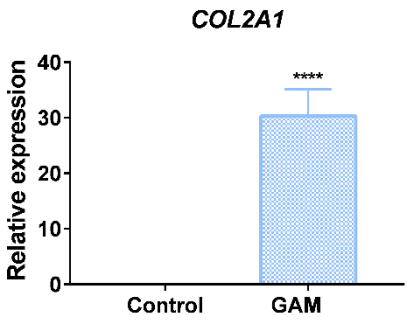

Figure S15. Gene expression of collagen type-2 after MSC encapsulation within SOX9-GAMs. One-way ANOVA was performed to compare gene expression levels ($P \leq 0.0001$) (n=3). Data represent the mean ±SD.